Makoqueta shale as radium source for the Cambro-Ordovician Aquifer in Eastern Wisconsin: final report submitted to the Wisconsin Department of Natural Resources. [DNR-141] 2000

Grundl, Timothy J., 1953-
[Wisconsin]: [Wisconsin Department of Natural Resources], 2000

https://digital.library.wisc.edu/1711.dl/U2DQNIRX5QJCY8L

Makoqueta Shale as Radium Source for the Cambro-Ordovician Aquifer in Eastern Wisconsin

by
Tim Grundl

141
051416

Makoqueta Shale as Radium Source for the Cambro-Ordovician Aquifer in Eastern Wisconsin

Tim Grundl
Associate Professor
Geosciences Department
University of Wisconsin - Milwaukee

Final Report submitted to the Wisconsin Department of Natural Resources
December 20, 2000

Table of Contents

INTRODUCTION

This project was designed to investigate the extent and source of radium contamination in the Cambro-Ordovician aquifer system of eastern Wisconsin. Extensive use was made of the test well installed by the Wisconsin Geological and Natural History Survey (WGNHS) at Minooka Park, Waukesha, Wisconsin. Funding for the project was provided through the Wisconsin Department of Natural Resources (WDNR). We would also like to acknowledge the help of Tim Eaton of the WGNHS and the support staff at the Great Lakes WATER Institute. Derek Clayton and Mike Cape were the student research assistants who did the field and laboratory analytical work.

BACKGROUND AND OBJECTIVES

The Cambro-Ordovician aquifer system in eastern Wisconsin is becoming ever more heavily relied upon as a source of drinking water by many of the rapidly growing urban centers of eastern Wisconsin. The water produced from this aquifer often contains combined radium activities in excess of the drinking water limit of 5 pCi/L, in some cases in excess of 30 pCi/L. Because the source of this radium is not fully understood, basic questions as to how best to manage this increasingly important source of drinking water are unanswerable. Previous studies have shown that radium concentrations in excess of approximately 5 pCi/L are not supportable by the presence of parent isotopes in the aquifer solids. Furthermore a spatial correlation exists between the occurrence of high radium in Cambro-Ordovician groundwater and the bedrock subcrop pattern of the Makoqueta Shale. It is therefore possible that high radium concentrations in Cambro-Ordovician water originate from downward flow of recharge water through the Makoqueta Shale. Hydrologic conditions prevailing in the Cambro-Ordovician aquifer are consistent with this hypothesis. The Makoqueta outcrop pattern forms the demarcation between unconfined conditions in the underlying Cambro-Ordovician aquifer to the west and confined conditions to the east. Strong downward gradients exist across the Makoqueta and flow across the unit should be maximal near the outcrop where total thickness is at a minimum. This strong downward gradient is very recent and is caused by heavy pumpage of the Cambro-Ordovician in urban areas. The objectives of this study were to:

1) Define the extent of the radium problem within the Cambro-Ordovician aquifer. Specifically, the extent of high radium groundwater within the Cambro- Ordovician aquifer is to be defined in both the spatial and temporal domains. This was done by making extensive use of both water quality and well construction data contained in the WDNR Drinking Water Database.

2) Determine if the Makoqueta Shale serves as the source for the high radium content observed in portions of the Cambro-Ordovician aquifer. This objective was studied by measuring the levels of both radium and the parent isotopes in the Makoqueta solids. The radium content of water produced by the Makoqueta was also determined. Lastly, the radium content of water produced from the uppermost unit of the Cambro-Ordovician aquifer (the Galena-Platteville Dolomite) was to be measured. This information allowed an estimation to be made of the level of radium input, if any, to the top of the Cambro-Ordovician aquifer.

The geochemistry of the two radium isotopes and their parent isotopes are quite different. The ^{226}Ra decay chain is shown in Figure 1. There are three important parent isotopes, ^{238}U, ^{234}U and ^{230}Th. The ^{228}Ra decay chain is very simple with the ultimate parent ^{232}Th decaying directly to ^{228}Ra. (Figure 2). Thorium is essentially insoluble in oxic freshwaters and can be considered immobile. Uranium forms the uranyl ion (UO_2^{2+}) in oxic waters. Uranyl sorbs strongly to ferric oxides and is relatively immobile. Uranyl does complex to carbonate ions to form $UO_2CO_2^{\circ}$ ion pairs. In this form, uranium is highly mobile. In anoxic waters, uranium forms the uranous (U^{4+}) ion and is very insoluble. Therefore carbonate rich, oxic waters promote the mobility of uranium. Radium exists largely as the free ion (Ra^{2+}). Ra^{2+} readily sorbs to iron oxides and tends to co-precipitate into the sulfate minerals barite and gypsum. As a rule, in aquifer systems the bulk of the radioactivity is housed on the solids present, not in the aquifer fluids.

METHODS

Sample analysis of aquifer solids was performed at the Great Lakes WATER Institute. Uranium and thorium content was measured by alpha spectroscopy. Solids were pulverized and subjected to sequential extraction. Samples were extracted using 6M hydrochloric acid to separate surface coatings from the underlying silicate minerals. Silicate minerals were extracted using a mixture of hydrofluoric and nitric acid. Carbonate material was also dissolved during the first extraction step, but carbonate minerals themselves do not contain significant amounts of radioactivity. Both extracts were analyzed separately for the parent isotopes of radium, ^{238}U, ^{234}U, ^{230}Th, and ^{232}Th. This extraction procedure allowed the examination of parent isotope distribution in the surface coatings versus that in the underlying silicate minerals. Uranium and thorium isotopes were separated by dripping extracts through anion exchange columns and electroplating the radioisotopes onto stainless steel discs. The discs were counted in an alpha spectrometer. ^{226}Ra was determined in the bulk solids via radon emanation. Samples were placed in a sealed container for a minimum of three weeks until secular equilibrium between radium and radon was reached. Radon activity of the extracted gas was counted in a Lucas chamber. A full description of analytical protocols can be found in Clayton (1999). Radiometric content of Minooka Park well water was performed at the Wisconsin State Laboratory of Hygiene.

RESULTS

Spatial and temporal extent of radiometric content of Cambro-Ordovician water

The WDNR Drinking Water database served as the source for all radiometric data used in the following discussion. At any given municipality, radiometric data is typically measured in the distribution system. Well-specific data is very sparse. The WDNR database was filtered such that only public water supply systems that obtain their water solely from the Cambro-Ordovician aquifer were used. This eliminated systems with mixed Silurian and Cambro-Ordovician water supplies, however the generic lack of well- specific data does not allow the effects of mixing of several Cambro-Ordovician wells within a distribution system to be eliminated. The advantage of using distribution system data is that it does give information as to the radiometric content of water that is being consumed by the public.

Figures 3 through 5 depict the average total radium ($^{226}Ra + ^{228}Ra$) concentrations seen in public water supply systems in 5-year increments starting in 1986 and ending in 2000. Figure 6 shows the location of the water supply systems used to generate these figures. In general, radium activities remain relatively constant in the southeast comer of the state with perhaps a small increase in the area containing greater than 10 pCi/L within Waukesha county. The concentrations in Calumet County appear to decline somewhat over this period of time. A clear band of high radium concentrations is seen that is roughly parallel to the subcrop pattern of the Makoqueta Shale (shown in the shaded area). The location of this band does not vary over time.

Figures 7 through 9 depict the average gross alpha concentrations seen in the same public water supply systems in 5-year increments starting in 1986 and ending in 2000. Gross alpha also occurs along a band that is roughly parallel to the Makoqueta Shale subcrop, however there are high gross alpha wells to the west of the subcrop in Winnebago County and to the east of the subcrop in Waukesha, Milwaukee and Kenosha counties. In contrast to radium, gross alpha activities show a clear increase over time throughout the region. In 1986-1990, the maximum activity in southeast portion of the state (Waukesha County) was 17 pCi/L, while in 1995-2000 the maximum rose to 39 pCi/L. A similar trend occurs in the northeast portion of the state (Brown County) with maximum activities rising from 44 to 74 pCi/L during the same time periods.

Gross alpha radiation is generally considered to arise from precursor isotopes of radium, chiefly uranium and thorium, although recent evidence suggests that gross alpha may arise from short lived daughter products of radium, chiefly polonium. (Sonzogni 2000). In either case, the geochemical behavior of those isotopes responsible for gross alpha is different from radium.

Geochemistry of the Makoqueta Shale

The clear relationship between the Makoqueta Shale subcrop and radiometric content of the underlying water leads to the suggestion that the Makoqueta Shale is either the direct source of radioactivity, or is indirectly causing high radioactivity. To investigate these possibilities, a detailed study of the geochemistry of the Makoqueta Shale was undertaken. Makoqueta drill cuttings were obtained from three wells (Franklin well #5, Lac La Belle, and Oakfield well #3) and core samples were obtained from a fourth well (Minooka Park well). Franklin #5 is a large municipal well that is open to the entire Cambro-Ordovician aquifer and produces water with 6-8 pCi/L total radium. Lac La Belle was an irrigation well that extended only 5 feet into the Cambro-Ordovician system. Oakfield #3 was a municipal well that produced 10-15 pCi/L total radium along with high sulfate and for this reason has been abandoned. The Minooka Park well is a research well installed by the WGNHS that is open to the Makoqueta Shale and the top 30 feet of the underlying Galena-Platteville Dolomite.

Figure 10 shows the location of the Franklin #5, Minooka Park and Lac La Belle wells. These wells form a transect that extends across the Makoqueta Shale from very near the westernmost limit (Lac La Belle) southeast to Franklin #5. Samples were collected from all three stratigraphic units within the Makoqueta in all wells except Lac La Belle. Lac La Belle is very near the pinchout of the Makoqueta and only the Scales Shale unit is present. The complete sample set is representative of the entire vertical extent of the Makoqueta and the lateral extent from the pinchout to well within the eastern portion of the unit. Figure 11A is a diagrammatic representation of the lateral stratigraphy along the transect. The stratigraphy of the Makoqueta Shale is shown diagrammatically in Figure 11B. Table 1 lists the average isotopic concentration for both surface and silicate fractions within each stratigraphic unit of the Makoqueta. The full isotopic data table is given in Appendix A. As expected, the concentration of all isotopes was smallest in the Fort Atkinson member of the Makoqueta. This is due to the high carbonate content of the Fort Atkinson.

Information consistent with the idea that radioisotopes in the solids of the Makoqueta are being mobilized by groundwater movement can be found by examination of the $^{234}U/^{238}U$ activity ratios. ^{234}U enrichment is commonly observed in groundwaters because of alpha recoil and selective leaching mechanisms (eg. Edgington, et al., 1996; Fleischer, 1980). When ^{238}U decays, the daughter isotope (^{234}U) is preferentially forced into the water by recoil from the ejected alpha decay particle. This mechanism also damages the lattice structure of the mineral and allows selective leaching of ^{234}U at the site. In the Makoqueta solids, the $^{234}U/^{238}U$ activity ratio of the surface coatings shows an enrichment in ^{234}U (i.e. the ratio is greater than one). The silicate fraction

		SURFACE FRACTION				SILICATE FRACTION			
Sample Description	Sample depth (feet)	^{238}U (dpm/g)	^{234}U	^{230}Th	^{232}Th	^{238}U (dpm/g)	^{234}U	^{230}Th	^{232}Th
Minooka well									
BR	259	17.75	21.20	4.52	10.38	5.08	3.52	1.82	0.95
FA	331	1.48	2.00	1.35	1.20	4.10	3.83	3.13	0.57
SS	375	1.39	2.92	4.70	8.79	2.00	1.22	0.94	0.85
Franklin #5 well									
BR	320	3.52	7.76	1.92	13.06	1.86	1.68	1.07	0.67
FA	415	1.02	2.62	1.25	2.72	4.00	2.90	2.76	1.20
SS	500	4.79	6.85	4.98	10.98	2.45	1.70	1.29	1.51
GP	530	0.13	0.54	1.64	0.43	18.51	25.63	6.41	7.22
Lac La Belle well									
SS	105	2.71	6.52	6.84	13.09	5.09	3.43	4.00	3.47
SS	115	2.53	4.61	8.17	13.35	6.09	3.91	4.03	2.08
Oakfield #3 well									
BR	55	1.39	1.89	4.40	10.71	3.14	2.63	0.62	0.64
FA	100	0.70	1.22	0.29	2.21	1.59	1.54	1.54	1.83
SS	230	3.18	5.05	5.88	13.88	4.40	3.21	2.42	2.57

Table 1: Average isotopic concentration for surface and silicate fractions within each stratigraphic unit of the Makoqueta Shale. Units are disintegration per minute (dpm) per gram of extracted mineral. BR = Brainard Shale. FA = Fort Atkinson Formation. SS = Scales Shale. GP = Galena Platteville Formation.

in each sample shows a corresponding depletion in ^{234}U (i. e. the ratio is less than one). The fact that surface coatings exhibit ^{234}U enrichment indicates that these coatings precipitated from similarly enriched water leaving the remaining silicate fraction depleted in ^{234}U. $^{234/238}U$ activity ratios are depicted in the vertical axis of the two cross-plots shown in Figure 12. Without exception, the silicate fraction (Figure 12B) falls below a $^{234}U/^{238}U$ activity ratio of one. All samples are clustered rather tightly together, indicating only small departures from secular equilibrium. In contrast, the surface coatings exhibit $^{234}U/^{238}U$ activity ratios greater than one and exhibit a large spread in both $^{234}U/^{238}U$ and $^{230}Th/^{238}U$ ratios (Figure 12A). This large spread is indicative of the differing extents of leaching that precedes the precipitation of surface coatings.

Another activity ratio trend that is consistent with the idea that radioisotopes are being mobilized in the Makoqueta can be seen by examination of the $^{230}Th/^{238}U$ activity ratios. Thorium is a very insoluble element that is unaffected by the leaching action of percolating groundwater. As groundwater leaches the more mobile uranium, the $^{230}Th/^{238}U$ activity ratio increases. More highly leached areas will exhibit higher $^{230}Th/^{238}U$ activity ratios. The Scales Shale is the only unit within the Makoqueta that was sampled in all three wells of the east-west transect. When this is done, it can be seen that the highest $^{230}Th/^{238}U$ ratios occur to the west (Lac la Belle) and decrease towards the east (Franklin #5). The circled points in Figure 12A represent samples collected from the Scales Shale. The Lac La Belle point with a $^{230}Th/^{238}U$ activity ratio of 2.5 was collected from the very top of the section and is not representative of the Scales Shale as a whole.

Aqueous chemistry of Makoqueta water

A detailed examination of the Makoqueta water as contained in the Minooka Park well was also performed. Extensive analyses of water samples previously collected from the Minooka Park well by WGNHS personnel have been published (Eaton and Bradbury, 1998). Water samples collected during the course of the current study matched this earlier WGNHS data except in those intervals where the packers had begun to leak. For this reason, the WGNHS data was used for the examination of Makoqueta water.

The stable isotopic signature of Makoqueta water provides evidence as to the flow patterns in the Makoqueta. The isotopic composition of virtually all meteoric water falls along the "meteoric water line" (see Figure 13) (Dansgaard, 1964). Any variation in isotopic signature along the meteoric line is because water becomes increasingly depleted in both ^{18}O and deuterium in colder climates. If a groundwater falls along the meteoric water line, it can be presumed that the isotopic signature reflects its meteoric origins. The temperature dependence of oxygen isotope ratio can be expressed by (Dansgaard, 1964):

$$^{18}O\ (‰) = 0.695(t) - 13.6$$

where t = average climatic temperature °C).

By using this equation, the isotopic signature of groundwater can be related to the average climatic conditions at the time of groundwater recharge (Perry, et al., 1982).

The average ^{18}O composition of modern meteoric water in southern Wisconsin is approximately $^{18}O = -7$ ‰. Table 2 and Figure 13 show the isotopic values for the Minooka waters. It is clear that there is a significant source of isotopically depleted water in the Makoqueta.

port number	stratigraphic unit	delta 18O ‰	delta D ‰	percent Pleistocene
7	Silurian	-8.58	-64.37	27
6	Fort Atkinson	-10.38	-76.35	51
5	Brainard (top)	-12.44	-94.76	65
4	Brainard (bottom)	-9.69	-71.66	100

Table 2. Stable isotopic composition of Minooka Park well water. Data taken from Eaton and Bradbury (1998).

This isotopically depleted water originated as recharge in a colder climate than exists at present. It is probable that the Makoqueta water is a mix of isotopically light water recharged during the Pleistocene glaciation and isotopically heavy water originating as modem day recharge. The isotopically lightest water, with an ^{18}O value of -12.44‰, is seen in the bottom of the Brainard. This isotopic signature matches the signature of the lightest water seen in previous studies (Perry, et al. 1982). Water with this isotopic signature originated in a climate with an average temperature of 2 °C (calculated from the temperature relation given above). The "percent Pleistocene" component seen in Table 2 and Figure 13 is based on the assignment of 100% Pleistocene to Brainard (bottom). Modern precipitation was assigned an $^{18}0$ value of -7 ‰. This interpretation is consistent with "modern" water moving slowly through the Makoqueta. Fort Atkinson water has a relatively low Pleistocene percentage (51 %) for its position in the stratigraphic sequence, indicating that it is a primary conduit for water flow. The top of the Brainard has a value of 65% Pleistocene suggesting influx of modern water from the reversal of hydraulic gradient across the Makoqueta due to heavy pumping of the underlying Cambro-Ordovician aquifer. No reliable stable isotopic data exists for the ports open to the Scales Shale or Galena-Platteville formations (Eaton, personal communication). The presence of Pleistocene-age water in portions of the Makoqueta is consistent with previous travel time estimates through the Makoqueta (Eaton and Bradbury, 1998; Weaver and Bahr, 1991a, b).

The chemical evolution in the major ion chemistry of groundwater as it passes through the Makoqueta is typical for that seen in other subsurface flow systems. The overlying Silurian Dolomite water (Minooka port 7) is a typical southeastern Wisconsin Ca-Mg-HCO_3 water. As the water moves downward through the Makoqueta to the Fort Atkinson and then to the Scales Shale, the ionic signature becomes strongly Na-HCO_3. Sodium concentrations rise at the expense of calcium and magnesium. Bicarbonate concentrations also rise along the flowpath. The increasing sodium signature is not due to halite dissolution because there is no corresponding rise in chloride concentrations. This geochemical evolution is due to the microbial oxidation of organic carbon and the concomitant production Of CO_2 gas which yields acidity in the form of carbonic acid ($H_2CO_3^o$).

Carbonic acid dissolves the dolomite present in these sediments, releasing Ca^{2+} and Mg^{2+} ions. These ions are exchanged onto clay minerals, yielding two monovalent Na^{+} ions for each divalent ion. The mass balance equation for these processes is:

$$mCO_2 = \Delta M_{HCO3} - \Delta M_{Ca} - \Delta M_{Mg} - (\Delta M_{Na} + \Delta M_{Cl})/2$$

where mCO_2 = moles CO_2 gas produced from organic carbon oxidation
ΔM_{Na} = change in molarity of Na along flowpath.

This geochemical evolution through time can be observed on Figure 14. This plot indicates that Ca-Mg-HCO_3 water from the Silurian (port 7) is moving through the Fort Atkinson and into the upper portions of the Brainard Shale (ports 3,4 and 6). The lower portion of the Brainard Shale, the Scales Shale and the Galena-Platteville (ports 1,2,and 5) have fully evolved towards a Na-HCO_3 character. The rate of carbon oxidation can be estimated from the difference in ion content of Silurian Dolomite (port 7) water and Scales Shale water (port 2) by assigning a travel time for water movement through the Makoqueta. The stable isotopic data discussed above suggests that Pleistocene water (ca. 12,000 years old) remains in the Scales Shale. Weaver and Bahr (199la, b) calculate a residence time of about 5600 years in the Makoqueta. These two travel time estimates yield rates of 6E-4 to 1.3E-3 mMol/yr organic carbon oxidized. This oxidation rate matches literature values for carbon oxidation rates in deep aquifer systems which range from 1E-3 to 1E-6 mMol/L (Chapelle and Lovely, 1990).

It is interesting to note that Fort Atkinson water closely resembles the overlying Silurian recharge water. This is additional evidence that water is moving through the Fort Atkinson with little time for geochemical evolution. The top of the Brainard (Port 6) also contains water that has not had time to fully evolve. This trend matches the stable isotopic data and tends support to the idea that Silurian water is moving into the upper reaches of the Brainard due to the reversal of hydraulic gradient across the Makoqueta from heavy pumping of the underlying Cambro-Ordovician aquifer. The strong Na-HCO_3 nature of the Galena-Platteville water seems to indicate that Makoqueta water has moved downward into the underlying Galena-Platteville formation (port 1).

Against this geochemical backdrop, the ^{228}Ra and ^{226}Ra content of water collected from the Fort Atkinson, the Scales Shale and the Galena-Platteville in the Minooka Park well was measured. The results show that, in spite of the considerable radium content in the solids, and the obvious through 1999) and as such represents a "snapshot" of the current chemical conditions in the Cambro-Ordovician. Figure 15 shows the included municipalities. In the Cambro-Ordovician aquifer, there is a large cone of depression centered between Brookfield and Waukesha and water flows radially towards the center of this cone. The 14 municipalities were arranged along the groundwater flowpath according to their position with respect to the Makoqueta subcrop (gray in Figure 15). Table 4 lists the chemical data for these 14 municipalities. In this table and in the following figures, municipalities located to the west of the subcrop are assigned negative distances and municipalities located to the east of the subcrop are assigned positive distances.

When chemical conditions along this flowpath are examined, several interesting spatial trends emerge. There is a marked change in the anionic content of the water as it crosses the Makoqueta boundary (Figure 16). This mostly caused by an increase in sulfate, although bicarbonate steadily decreases along the flowpath. PHREEQC calculations of mineral saturation indices are shown in Figure 17. Carbonate minerals (calcite and dolomite) are slightly oversaturated throughout the system. This is likely due to continued bacterial CO2 production in the aquifer. Dolomite remains more oversaturated than calcite because of kinetic limitations on dolomite dissolution. The presence of the overlying Makoqueta has no apparent effect on carbonate saturation. In contrast, gypsum is undersaturated everywhere in the system by nearly two orders of magnitude. In this case, the presence of overlying Makoqueta does influence saturation state. There is a clear increase in saturation to the east of the Makoqueta subcrop.

The most interesting spatial trend shows that barite, within the accuracy of the calculations, is exactly in equilibrium everywhere in the system This is in spite of large variations in the sulfate concentration. One possible solid phase source of radium is the co-precipitation in sulfate minerals, in particular barite. There is a good co-variance of radium and barium concentrations to the west of the Makoqueta outcrop suggesting that barite dissolution is a possible source of radium in the unconfined portion of the aquifer (Figure 18). To the east of the Makoqueta, radium and barium no longer co-vary. This suggests that another source of radium is in operation. One possible source is the reductive dissolution of ferric hydroxides. The reductive dissolution of ferric hydroxides has previously been suggested, but with little data to back it up (Siegel, 1989).

The WDNR database was also examined to determine if there are any temporal trends in the chemistry of Cambro-Ordovician water. Although the database contains temporal data on radiometric constituents, temporal data on major ion chemistry is limited to a handful of isolated wells. Within a given municipality, two distinct trends over time are observed in the radiometric data. The first trend shows both the radium and gross alpha levels remaining constant over time. Cities that exhibit this trend include Horicon, Mayville, Campbellsport, Oakfield, Jefferson, Johnson Creek, Lake Mills, Franklin, Waterford, Union Grove, Elkhorn, Germantown, Pewaukee and Winneconne. An example can be seen in the city of Pewaukee. Figure 19 shows both gross movement of water through the Makoqueta, very little radium is being transferred to the water (Table 3).

	^{226}Ra water (pCi/L)	^{228}Ra (water) (pCi/L)	^{226}Ra Filtrate (pCi/kg)
Brainard Shale	--	--	--
Fort Atkinson	1.2	0.7	265
Scales Shale	0.32	ND	1660
	0.51	0.6	524
Galena-Platteville	*0.24*	*0.3*	--

Table 3. Radium content of filtered water taken from the Minooka Park well. Values for radium on solids is from filtrate of the respective water samples. Galena-Platteville data (in italics) is suspect because the packer immediately above had begun to leak.

These waters were filtered prior to analysis and the ^{226}Ra content of the filtrate was also measured. The data in Table 3 can be used to calculate the ^{226}Ra sorption coefficient (Kd) between Makoqueta water and the suspended solids. The log Kd value is 3.37 (±0.31) which is typical of literature values.

Results of the geochemical study indicate that groundwater is moving through the Makoqueta Shale and that radioactivity is being mobilized from the silicate minerals to the surface coatings. Furthermore, these phenomenon are more pronounced to the west (near the subcrop) where water movement is at a maximum. However, the one set of Makoqueta waters that were analyzed exhibit rather low radium content. The critical data point at the very top of the Cambro-Ordovician aquifer (Galena-Platteville) is not representative of actual conditions in the Galena-Platteville because at the time of sampling, the lowermost packer had lost it's seal. In spite of the fact that radioactivity is being mobilized within the Makoqueta, it is not possible to unequivocally state that the Makoqueta is directly supplying radium to the underlying Cambro-Ordovician aquifer.

Chemistry of Cambro-Ordovician water

It is possible that chemical changes within the Cambro-Ordovician aquifer caused by the Makoqueta are contributing to the mobilization of radium. To further investigate this possibility, the chemistry of water being pumped from a set of 14 municipalities in southeastern Wisconsin was extracted from the WDNR database and investigated in detail. These municipalities were chosen by virtue of their location with respect to the Makoqueta subcrop, and the availability of recent water quality data. This is a compendium of the major ion chemistry for a single time period (1997

MUNICIPALITY	Distance to Mako. (km)	pH	Ca^{2+}	Mg^{2+}	Na^{+}	Fe^{2+}	HCO_3^{2-} (mg/L)	Cl^{-}	SO_4^{2-}	NO_3^{-}	Ba^{2+}	Total Radium (pCi/L)	Gross Alpha (pCi/L)
Lake Mills	-25.2	7.6	59.7	42.7	3.6	0.2	361.0	1.9	20.0	0.0	0.079	4.4	11.0
Jefferson	-17.4	7.5	55.0	33.7	5.7	0.5	283.3	7.3	16.3	0.0	0.086	4.7	13.3
Johnson Creek	-12.9	7.5	65.0	31.5	5.0	0.4	274.5	2.1	0.0	0.2	0.496	6.3	14.3
Watertown	-12.9	7.5	69.3	35.0	5.0	0.3	310.0	6.4	60.0	0.0	0.099	2.0	9.2
Oconomowoc	-7.3	7.5	65.0	37.6	13.5	0.4	288.3	21.6	16.2	2.4	0.129	0.9	3.4
Eagle	0	7.5	55.5	26.5	3.5	0.0	275.0	0.0	2.7	0.0	0.875	10.3	22.0
Mukwonago	0.3	7.7	48.3	22.0	6.2	0.6	220.0	2.3	24.0	0.0	0.096	11.2	39.0
Delafield	1.1	7.8	58.0	28.0	4.5	0.3	248.0	3.2	15.0	0.1	0.130	5.7	13.7
Waukesha	1.1	7.4	88.0	24.9	25.5	0.3	220.0	18.5	118.6	0.0	0.054	12.1	31.0
Pewaukee Village	2.2	7.7	51.8	27.3	9.4	0.3	247.5	1.5	55.0	0.0	0.101	6.3	12.4
City of Pewaukee	3.4	7.6	77.3	28.0	13.0	0.1	234.0	8.0	125.0	0.0	0.029	--	--
Brookfield	6.7	7.7	83.8	26.0	17.9	0.3	207.5	19.7	101.5	0.0	0.034	6.1	24.0
New Berlin	8.4	7.6	107.7	27.9	17.7	0.4	257.3	28.1	157.3	0.0	0.033	5.5	24.0
Franklin	11.2	7.6	89.5	22.8	17.3	0.9	255.0	7.4	129.8	0.0	0.026	2.8	10.2

Table 4. Representative major ion composition of water being pumped from southeastern Wisconsin municipalities during the period 1997 to 1999. Data obtained from the WDNR drinking water database.

alpha and radium activities in Pewaukee from 1982 to 1997. The heavy black line is the 3-year moving average. Neither gross alpha, ^{228}Ra nor ^{226}Ra show any trend over time. Major ion chemistry taken from Pewaukee well 4 in 1978 and 1989 shows no change in the major ion composition, consistent with an unchanging radiometric content. A different situation exists in the city of New Berlin in which the same unchanging radiometric content is seen, but there is a clear increase in Ca-SO_4 salinity(see Appendix B). This is probably due to the competing effects of an increase in salinity and an increase in sulfate. An increase in salinity will tend to remove radium from cation exchange sites because of increased competition from major cations (in this case Ca^{2+}). Conversely, an increase in sulfate will remove radium from the water by co-precipitation with barite.

The second commonly observed temporal trend has radium content remaining constant with a steadily increasing gross alpha content. Cities that exhibit this trend include Ashwaubenon, Bellevue, Howard, Hustisford, Waupan, Fond du Lac, Crestview, Whitewater, Brookfield, New Berlin, Sussex, and Waukesha. An example can be seen in the city of Brookfield. Fig 20 shows both gross alpha and radium activities in Brookfield from 1980 to 1999. The heavy black line is the 3-year moving average. The steady rise in gross alpha levels starting in 1990 is evident. Except for two anomalous ^{228}Ra values in 1996, the radium levels are constant. Major ion chemistry taken from Brookfield well 24 shows a 46% increase in HCO3- content between 1990 and 1999 (see Appendix B). If the increase in gross alpha content is assumed to arise from uranium isotopes (radium isotopes remaining steady), the observed increase in HCO3- could mobilize sufficient uranium to account for the observed rise in gross alpha.

CONCLUSIONS

This study has furthered the understanding of the geochemical and radiometric conditions within the Makoqueta Shale and the underlying Cambro-Ordovician aquifer system. The extent of high radioactivity in the Cambro-Ordovician has been defined in terms of both spatial extent and variations through time. Insights into the geochemical processes that are contributing to high radioactivity have also been elucidated. All of these results are consistent with and expand upon previous studies. A summary of the important results is given below.

1) High radium activity occurs in the Cambro-Ordovician in a band roughly coincident with the Makoqueta subcrop pattern. This pattern extends across the entire eastern portion of the state from Brown County in the north to Racine County in the south. Radium activities have remained relatively constant from the middle 1970s to the present.

2) High gross alpha activity also occurs in a band roughly coincident with the Makoqueta subcrop pattern extending along the entire eastern portion of the state. Gross alpha activity has been steadily rising from the middle 1970s to the present.

3) Stable isotope and major ion chemistry indicate that water is moving through the Makoqueta Shale. Major ion chemistry indicates that water is moving through the Fort Atkinson with little time for geochemical evolution. Stable isotope chemistry is also indicative of groundwater movement through the Makoqueta. Water with a Pleistocene isotopic signature remains in portions of the Makoqueta, consistent with slow passage of water.

4) Radioisotope ratios within the Makoqueta Shale indicate that radioisotopes are being mobilized from their original position in the silicate minerals to surface coatings. This mobilization is most pronounced near the westernmost extent of the Makoqueta where water movement is at a maximum. In spite of the fact that radioisotopes are being mobilized by moving groundwater, there is no direct evidence for high radium content in Makoqueta water. This result is based upon a single set of groundwater samples collected from the Minooka Park well.

5) The presence of the Makoqueta Shale causes changes in the major ion chemistry of the underlying Cambro-Ordovician, in particular an increase in SO_4^{2-} at the expense of HCO_3^-. Limited data indicate that other subtle changes are occurring over time in the Cambro-Ordovician that could be the cause of high radioactivity near the subcrop pattern of the Makoqueta. There are indications that radium content to the west of the Makoqueta subcrop is largely controlled by dissolution of barite. To the east of the subcrop other processes are likely in operation. These could include reductive dissolution of ferric hydroxides, cation exchange reactions, or mobilization of the parent isotopes of uranium. Specific wells can be found to indicate that one or more of these processes is occurring locally.

In any given aquifer system, the bulk of the radioactivity will reside on the solids, not in the aqueous phase. Determining which process(es) control the release of solid- phase radioactivity in the Cambro-Ordovician into the groundwater will require a more thorough understanding of the system. The actual cause for high radium and gross alpha activities in the Cambro-Ordovician is undoubtedly a combination of multiple, sometimes subtle, processes that may differ from location to location. The largest gap in our understanding of the Cambro-Ordovician is the lack of vertically discrete chemical information caused by the fact that deep sandstone wells are screened across large portions of the aquifer. There is essentially no information as to the spatial extent of high radioactivity in the vertical direction. The paucity of major ion chemistry over time represents another gap in our understanding. This limits our ability to model the underlying causes behind the trends in the radiometric content. Future research efforts should focus on developing vertically discrete information and the initiation of a long- term program to monitor changes in major ion chemistry.

REFERENCES

Chapelle, F. and Lovely, D. 1990. Rates of microbial metabolism in deep coastal plain aquifers. Appl. Environmental Microbiol. 56(6):1865-1874.

Clayton, D. 1999. Radioisotopes in the Makoqueta Formation. UWM Master's thesis. 102 pp.

Dansgaard, W. 1964. Stable isotopes in precipitation. Tellus 16(4):436-468.

Eaton, T., and Bradbury, K. 1998. Evaluation of the confining properties of the Makoqueta Formation in the SEWRPC region of southeastern Wisconsin. Wisc. Geologic and Natural History Survey Open-File Report 1998-11. 34pp.

Edgington, D., Robbins, J., Colman, S., OriandinL K., Gustin, M. 1996. Uranium-series disequilibriuni, sedimentation, diatom ftustrules, and paleoclimatic change in Lake Baikal. Earth Planet. Sci. Letters. 142:29-42.

Fleischer, R.L. 1980. Isotopic disequilibriurn of Uranium: Alpha-recoil damage and preferential solution effects. Science 207(29):979-981.

Perry, G., Grundl, T. and Gilkeson, R. 1982. H,O, and S isotopic study of the Cambro-Ordovician aquifer system of northern Illinois. *in* Perry and Montgomery, eds. Isotope Studies of Hydrologic Processes. NIU Press pp.35-43.

Siegel, D. 1989. Geochemistry of the Cambro-Ordovician aquifer system in the northern midwest, United States. USGS Prof. Paper 1405-D. 75 pp.

Sonzogni, B. B. 2000. Naturally occurring radioactivity in groundwater. Presentation at the WDNR Drinking Water Supply Statewide Meeting, La Crosse. Sept. 28, 2000.

Weaver, T. and Bahr, J. 1991a. Geochemical evolution of the Cambro-Ordovician aquifer, eastern Wisconsin: 1. Major ion and radionuclide distribution. Ground Water 29:350-356.

Weaver, T. and Bahr, J. 1991b. Geochemical evolution of the Cambro-Ordovician aquifer, eastern Wisconsin: 2. Correlation between flow paths and ground water chemistry. Ground Water 29:510-515.

Appendix A: Raw isotopic data for samples of Makoqueta Shale solids. Bulk 1 values are from the surface fraction; Bulk 2 extracts are from the silicate fraction.

Uranium Concentrations

	^{232}Thorium	^{238}Uranium	^{234}Uranium
Decay Constants			
Decay Constants (per min)	9.414E-17	2.949E-16	5.34E-12
Molecular mass (g/Mole)	232	238	234
Avagadro's # (atoms/mole)	6.02E+23		
DPM/pCi	2.20E+00		

Bulk 1 = Carbonate Portion
Bulk 2 = Silicate Portion

	Date Counted	Total Recovery (%)	Amount Sampled	% Lost	DPM	DPM/g	ppm	pCi/g	$^{234}U/^{238}U$ Ratio	Total error
BR-231-U-Bulk 1	3/2/99	21.48	0.4449	14	1.75E+00	2.83E+01	3.79E+01	1.29E+01	1.04E+00	1.47E-01
BR-231-U234-Bulk 1	3/2/99	21.48	0.4449	14	1.83E+00	2.95E+01	2.15E-03	1.34E+01		1.45E-01
BR-231-U-Bulk 2 Run 4	4/30/99	25.29	0.38	92	2.41E+00	6.88E+00	9.23E+00	3.13E+00	7.29E-01	1.43E-01
BR-231-U234-Bulk 1 Run 4	4/30/99	25.29	0.38	92	1.76E+00	5.02E+00	3.65E-04	2.28E+00		1.54E-01
BR-287-U Bulk 1	4/7/99	31.95	0.4449	14	4.48E-01	7.22E+00	9.68E+00	3.28E+00	1.78E+00	2.06E-01
BR-287-U234 Bulk 1	4/7/99	31.95	0.4449	14	7.98E-01	1.29E+01	9.37E-04	5.85E+00		1.65E-01
BR-287-U Bulk 2	3/31/99	29.57	0.4449	86	1.25E+00	3.27E+00	4.38E+00	1.49E+00	6.16E-01	2.40E-01
BR-287-U234 Bulk 2	3/31/99	29.57	0.4449	86	7.69E-01	2.01E+00	1.47E-04	9.15E-01		2.83E-01
FA-317-U-Bulk 1	3/1/99	32.69	1.051	93	2.69E+00	2.75E+00	3.69E+00	1.25E+00	1.23E+00	1.66E-01
FA-317-U234-Bulk 1	3/1/99	32.69	1.051	93	3.31E+00	3.39E+00	2.47E-04	1.54E+00		1.58E-01
FA-317-U-Bulk 2	4/26/99	21.32	0.482	6.4	1.21E-01	3.93E+00	5.27E+00	1.79E+00	1.07E+00	3.31E-01
FA-317-U234-Bulk 2	4/26/99	21.32	0.482	6.4	1.29E-01	4.20E+00	3.06E-04	1.91E+00		3.21E-01
FA-331-U Bulk 1	3/2/99	32.22	0.791	75	1.83E-01	3.08E-01	4.14E-01	1.40E-01	1.33E+00	2.62E-01
FA-331-U234 Bulk 1	3/2/99	32.22	0.791	75	2.43E-01	4.10E-01	2.98E-05	1.86E-01		2.30E-01
FA-331-U Bulk 2	3/13/99	21.48	0.791	22	7.48E-01	4.27E+00	5.73E+00	1.94E+00	8.11E-01	2.32E-01
FA-331-U234 Bulk 2	3/13/99	21.48	0.791	22	6.06E-01	3.46E+00	2.52E-04	1.57E+00		2.51E-01
FA-345-U Bulk 1	3/11/99	34.10	1.157	30	4.75E-01	1.37E+00	1.84E+00	6.23E-01	1.60E+00	2.76E-01
FA-345-U234 Bulk 1	3/11/99	34.10	1.157	30	7.60E-01	2.19E+00	1.59E-04	9.96E-01		2.38E-01
SS-358-U BULK1	4/6/99	9.64	0.5854	31	2.38E-01	1.32E+00	1.76E+00	5.98E-01	2.11E+00	3.54E-01
SS-358-U234 BULK 1	4/6/99	9.64	0.5854	31	5.04E-01	2.78E+00	2.03E-04	1.26E+00		2.68E-01
SS-358-U BULK 2	4/6/99	35.56	0.5854	65.5	8.97E-01	2.34E+00	3.14E+00	1.07E+00	6.11E-01	2.90E-01
SS-358-U234 BULK 2	4/6/99	35.56	0.5854	65.5	5.48E-01	1.43E+00	1.04E-04	6.51E-01		3.36E-01
SS-392-U Bulk 1	2/25/99	16.01	0.994	30	4.37E-01	1.46E+00	1.96E+00	6.66E-01	2.09E+00	2.94E-01
SS-392-U234 Bulk 1	2/25/99	16.01	0.994	30	9.11E-01	3.06E+00	2.23E-04	1.39E+00		2.33E-01
SS-392-U Bulk 2	3/13/99	32.20	0.994	70	1.15E+00	1.66E+00	2.22E+00	7.54E-01	6.11E-01	1.55E-01
SS-392-U234 Bulk 2	3/13/99	32.20	0.994	70	7.04E-01	1.01E+00	7.37E-05	4.60E-01		5.26E-01
FR-320-U-Bulk 1 Dup	2/23/99	38	0.538	12	2.52E-01	3.88E+00	5.20E+00	1.76E+00	2.00E+00	5.86E-01
FR-320-U234-Bulk 1 Dup	2/23/99	38	0.538	12	5.04E-01	7.76E+00	5.65E-04	3.53E+00		5.77E-01
FR-320-U-Bulk 1 Run 3	4/18/99	26.75	0.422	25	3.32E-01	3.16E+00	4.24E+00	1.44E+00	1.59E+00	2.80E-01
FR-320-U234-Bulk 1 run 3	4/18/99	26.75	0.422	25	5.29E-01	5.04E+00	3.67E-04	2.29E+00		2.31E-01
FR-320-U-Bulk 2	4/13/99	15.65	0.5203	0	9.70E-01	1.86E+00	2.50E+00	8.48E-01	9.01E-01	3.00E-01
FR-320-U234-Bulk 2	4/13/99	15.65	0.5203	0	8.74E-01	1.68E+00	1.22E-04	7.64E-01		3.09E-01
FR-415-U-Bulk 1 Duplicate	2/25/99	18.00	0.4568	57	3.66E-01	1.41E+00	1.89E+00	6.40E-01	1.45E+00	3.33E-01
FR-415-U234-Bulk1 Duplicate	2/25/99	18.00	0.4568	57	5.30E-01	2.04E+00	1.48E-04	9.27E-01		2.77E-01
FR-415-U-Bulk 1 Run 3	4/18/99	21.79	0.4104	57	2.39E-01	1.02E+00	1.37E+00	4.65E-01	2.57E+00	4.57E-01
FR-415-U234-Bulk1 Run 3	4/18/99	21.79	0.4104	57	6.14E-01	2.62E+00	1.91E-04	1.19E+00		3.24E-01
FR-415-U-Bulk 2 Run 3	4/21/99	28.09	0.4104	39	6.40E-01	4.00E+00	5.36E+00	1.82E+00	7.24E-01	1.59E-01
FR-415-U234-Bulk 2 Run 3	4/21/99	28.09	0.4104	39	4.63E-01	2.90E+00	2.11E-04	1.32E+00		1.81E-01
FR-485-U-Bulk 1	2/23/99	26.31	0.703	19	7.56E-01	5.68E+00	7.62E+00	2.58E+00	1.88E+00	1.75E-01
FR-485-U234-Bulk 1	2/23/99	26.31	0.703	19	1.42E+00	1.07E+01	7.78E-04	4.86E+00		1.42E-01
FR-485-U-Bulk 2	4/12/99	37.52	0.2838	0	5.40E-01	1.90E+00	2.55E+00	8.66E-01	7.79E-01	2.51E-01
FR-485-U234-Bulk 2	4/12/99	37.52	0.2838	0	4.21E-01	1.48E+00	1.08E-04	6.74E-01		2.73E-01
FR-515-U-Bulk 1 Run 3 Duplicate	2/25/99	27.67	1.358	24	1.12E+00	3.43E+00	4.60E+00	1.56E+00	1.71E+00	1.49E-01
FR-515-U234-Bulk 1 Run 3 Duplicate	2/25/99	27.67	1.358	24	1.92E+00	5.89E+00	4.29E-04	2.68E+00		1.28E-01
FR-515-U-Bulk 1 Run 3	4/18/99	20.97	0.4847	23	4.33E-01	3.89E+00	5.21E+00	1.77E+00	2.04E+00	2.78E-01
FR-515-U234-Bulk 1 Run 3	4/18/99	20.97	0.4847	23	8.82E-01	7.91E+00	5.76E-04	3.60E+00		2.11E-01
FR-515-U-Bulk 2 Run 4	4/13/99	13.53	0.2303	0	6.90E-01	3.00E+00	4.02E+00	1.36E+00	6.41E-01	2.39E-01
FR-515-U234-Bulk 2 Run 4	4/13/99	13.53	0.2303	0	4.42E-01	1.92E+00	1.40E-04	8.74E-01		2.76E-01
FR-530-U Bulk 1 run 3	4/28/99	18.43	0.312	96	2.69E-02	1.32E-01	1.77E-01	6.00E-02	4.07E+00	7.85E-01
FR-530-U234-Bulk 1 run 3	4/28/99	18.43	0.213	96	1.10E-01	5.37E-01	3.91E-05	2.44E-01		4.04E-01
FR-530-U-Bulk 2	4/7/99	25.74	0.557	1	1.03E-01	1.85E+01	2.48E+01	8.41E+00	1.38E+00	3.56E-01
FR-530-U234-Bulk 2	4/7/99	25.74	0.557	1	1.43E-01	2.56E+01	1.87E-03	1.16E+01		3.08E-01
OK-55-U BULK 1 Run 2	4/5/99	15.25	0.4995	37	2.53E-01	1.39E+00	1.86E+00	6.32E-01	1.36E+00	2.88E-01
OK-55-U234 BULK 1 Run 2	4/5/99	15.25	0.4995	37	3.44E-01	1.89E+00	1.38E-04	8.59E-01		2.52E-01
OK-55-U BULK 2 Run 2	4/14/99	28.03	0.4995	61	9.59E-01	3.14E+00	4.22E+00	1.43E+00	8.35E-01	1.57E-01
OK-55-U234 BULK 2 Run 2	4/14/99	28.03	0.4995	61	8.01E-01	2.63E+00	1.91E-04	1.19E+00		1.67E-01
OK-100-U BULK 1(run 2	4/5/99	19.89	0.641	58	2.59E-01	6.97E-01	9.34E-01	3.17E-01	1.76E+00	2.62E-01
OK-100-U234 BULK 1 (run 2)	4/5/99	19.89	0.641	58	4.55E-01	1.22E+00	8.91E-05	5.56E-01		2.06E-01
OK-100-U BULK 2 (run 2)	4/14/99	31.18	0.641	39	3.98E-01	1.59E+00	2.13E+00	7.24E-01	9.69E-01	2.18E-01
OK-100-U234 BULK 2 (run 2)	4/14/99	31.18	0.641	39	3.86E-01	1.54E+00	1.12E-04	7.02E-01		2.20E-01
OK-230-U Bulk 1	4/5/99	27.53	0.5338	25	4.24E-01	3.18E+00	4.26E+00	1.45E+00	1.59E+00	2.88E-01
OK-230-U234 Bulk 1	4/5/99	27.53	0.5338	25	6.74E-01	5.05E+00	3.68E-04	2.29E+00		2.39E-01
OK-230-U Bulk 2	3/16/99	22.90	0.5338	71	1.67E+00	4.40E+00	5.90E+00	2.00E+00	7.29E-01	2.50E-01

Uranium Concentrations

Decay Constants	^{232}Thorium	^{238}Uranium	^{234}Uranium
Decay Constants (per min)	9.414E-17	2.949E-16	5.34E-12
Molecular mass (g/Mole)	232	238	234
Avagadro's # (atoms/mole)	6.02E+23		
DPM/pCi	2.20E+00		

Bulk 1 = Carbonate Portion
Bulk 2 = Silicate Portion

	Date Counted	Total Recovery (%)	Amount Sampled	% Lost	DPM	DPM/g	ppm	pCi/g	$^{234}U/^{238}U$ Ratio	Total error
OK-230-U234 Bulk 2	3/16/99	22.90	0.5338	71	1.22E+00	3.21E+00	2.33E-04	1.46E+00		2.75E-01
LLB 105 U BULK 1	4/10/99	19.83	0.6163	32	5.23E-01	2.71E+00	3.64E+00	1.23E+00	2.40E+00	2.83E-01
LLB 105 U234 BULK 1	4/10/99	19.83	0.6163	32	1.26E+00	6.52E+00	4.75E-04	2.96E+00		2.06E-01
LLB 105 U BULK 2	4/23/99	32.46	0.6163	65	2.04E+00	5.09E+00	6.83E+00	2.32E+00	6.73E-01	1.36E-01
LLB 105 U234 BULK 2	4/23/99	32.46	0.6163	65	1.37E+00	3.43E+00	2.50E-04	1.56E+00		1.52E-01
LLB 125 U BULK 1 Run 2	4/22/99	22.71	0.434	29	2.96E-01	2.35E+00	3.15E+00	1.07E+00	1.14E+00	2.26E-01
LLB 125 U234 BULK 1 Run 2	4/22/99	22.71	0.434	29	3.39E-01	2.69E+00	1.96E-04	1.22E+00		2.14E-01
LLB 125 U BULK 2 Run 2	4/21/99	21.85	0.434	67	1.77E+00	6.09E+00	8.16E+00	2.77E+00	6.42E-01	1.95E-01
LLB 125 U234 BULK 2 Run 2	4/21/99	21.85	0.434	67	1.14E+00	3.91E+00	2.84E-04	1.78E+00		2.23E-01

Thorium Concentrations

Decay Constants	^{232}Thorium	^{230}Thorium
Decay Constants (per min)	9.414E-17	1.71E-11
Molecular mass (g/Mole)	232	230
Avagadro's # (atoms/mole)	6.02E+23	
DPM/pCi	2.20E+00	

Bulk 1 = Carbonate Portion
Bulk 2 = Silicate Portion

	Date Counted	Total Recovery (%)	Initial Mass sampled	% Lost	DPM	DPM/g	ppm	pCi/g	total error
BR-231-Th-Bulk 1	3/2/99	34.23	0.4449	14	2.00E+00	3.22E+00	1.32E+01	1.47E+00	9.47E-02
BR-231-Th230-Bulk 1	3/2/99	34.23	0.4449	14	1.68E+00	2.70E+00	6.03E-05	1.23E+00	9.39E-02
BR-231-Th-Bulk 2 Run 3	4/19/99	30.41	0.42	85	3.27E-01	9.34E-01	3.82E+00	4.24E-01	2.53E-01
BR-231-Th230-Bulk 2 run 3	4/19/99	30.41	0.42	85	1.56E+00	4.46E+00	9.94E-05	2.03E+00	1.08E-01
BR-287-Th Bulk 1	3/21/99	38.08	0.4449	14	1.09E+00	1.75E+01	7.18E+01	7.97E+00	2.12E-01
BR-287-Th230 Bulk 1	3/21/99	38.08	0.4449	14	3.93E-01	6.34E+00	1.41E-04	2.88E+00	2.52E-01
BR-287-Th Bulk 2	3/31/99	37.61	0.4449	86	3.72E-01	9.75E-01	3.99E+00	4.43E-01	1.69E-01
BR-287-Th230 Bulk 2	3/31/99	37.61	0.4449	86	3.59E-01	9.41E-01	2.10E-05	4.28E-01	1.23E-01
FA-317-Th-Bulk 1	3/1/99	28.32	1.051	93	8.75E-01	8.96E-01	3.67E+00	4.07E-01	2.23E-01
FA-317-Th230- Bulk 1	3/1/99	28.32	1.051	93	1.76E+00	1.80E+00	4.01E-05	8.17E-01	1.41E-01
FA-317-Th-Bulk 2 Run 2	4/26/99	32.27	0.482	6.4	9.07E-03	2.95E-01	1.21E+00	1.34E-01	1.73E+00
FA-317-Th230- Bulk 2 Run 2	4/26/99	32.27	0.482	6.4	ND	ND	#VALUE!	#VALUE!	4.39E-01
FA-331-Th-Bulk 1	3/21/99	26.62	0.791	75	7.85E-01	1.32E+00	2.95E-05	6.01E-01	3.16E-01
FA-331-Th230-Bulk 1	3/21/99	26.62	0.791	75	3.60E-02	6.07E-02	2.48E-01	2.76E-02	2.99E-01
FA-331-Th-Bulk 2	3/1/99	27.46	0.791	22	2.68E-02	1.53E-01	3.42E-06	6.96E-02	1.50E+00
FA-331-Th230-Bulk 2	3/1/99	27.46	0.791	22	9.72E-01	5.56E+00	2.27E+01	2.53E+00	2.15E-01
FA-345-Th Bulk 1	3/16/99	23.65	1.157	30	5.39E-01	1.55E+00	6.36E+00	7.06E-01	2.76E-01
FA-345-Th230 Bulk 1	3/16/99	23.65	1.157	30	4.85E-01	1.40E+00	3.12E-05	6.35E-01	2.45E-01
FA-345-Th Bulk 2 run 2	4/26/99	27.80	0.4172	60	3.12E-01	1.25E+00	5.11E+00	5.67E-01	1.68E-01
FA-345-Th230 Bulk 2 Run 2	4/26/99	27.80	0.4172	60	1.75E-01	7.00E-01	1.56E-05	3.18E-01	1.29E-01
SS-358-Th BULK 1	4/6/99	39.68	0.5854	31	1.39E+00	7.55E+00	3.09E+01	3.43E+00	1.70E-01
SS-358-Th230 BULK 1	4/6/99	39.68	0.5854	31	8.41E-01	4.58E+00	1.02E-04	2.08E+00	1.78E-01
SS-358-Th BULK 2	4/8/99	30.34	0.5854	65.5	3.88E-01	1.01E+00	4.15E+00	4.60E-01	2.48E-01
SS-358-Th230 BULK 2	4/8/99	30.34	0.5854	65.5	3.28E-01	8.56E-01	1.91E-05	3.89E-01	1.87E-01
SS-392-Th-Bulk 1	3/1/99	37.92	0.994	30	2.99E+00	1.00E+01	4.11E+01	4.56E+00	1.11E-01
SS-392-Th230-Bulk 1	3/1/99	37.92	0.994	30	1.44E+00	4.82E+00	1.08E-04	2.19E+00	1.39E-01
SS-392-Th-Bulk 2	3/13/99	20.14	0.994	70	4.74E-01	6.81E-01	2.79E+00	3.10E-01	2.67E-01
SS-392-Th230-Bulk 2	3/13/99	20.14	0.994	70	7.13E-01	1.03E+00	2.29E-05	4.66E-01	1.76E-01
FR-320-TH-Bulk1 Run 3	4/18/99	23.65	0.422	25	1.37E+00	1.31E+01	5.34E+01	5.93E+00	1.35E-01
FR-320-TH230-Bulk 1 Run 3	4/18/99	23.65	0.422	25	2.02E-01	1.92E+00	4.29E-05	8.73E-01	2.05E-01
FR-320-TH-BULK 2 RUN 3	4/12/99	28.89	0.5203	0	3.51E-01	6.74E-01	2.76E+00	3.07E-01	2.30E-01
FR-320-TH230-BULK 2 RUN 3	4/12/99	28.89	0.5203	0	5.58E-01	1.07E+00	2.40E-05	4.88E-01	1.62E-01
FR-415-TH-Bulk 1 run 3	4/18/99	31.74	0.4104	57	6.36E-01	2.72E+00	1.11E+01	1.24E+00	2.79E-01
FR-415-TH230 Bulk 1 run 3	4/18/99	31.74	0.4104	57	2.93E-01	1.25E+00	2.79E-05	5.68E-01	2.74E-01
FR-415-TH-BULK 2	4/7/99	38.50	0.4568	39	2.14E-01	1.20E+00	4.93E+00	5.47E-01	2.57E-01
FR-415-TH230-BULK 2	4/7/99	38.50	0.4568	39	4.90E-01	2.76E+00	6.15E-05	1.25E+00	1.31E-01
FR-485-TH-Bulk 1	2/25/99	14.72	0.703	19	1.21E+00	9.13E+00	3.74E+01	4.15E+00	1.75E-01
FR-485-TH230-Bulk 1	2/25/99	14.72	0.703	19	5.67E-01	4.26E+00	9.51E-05	1.94E+00	2.16E-01
FR-485-TH-Bulk 2	4/13/99	26.45	0.2838	0	3.36E-01	1.18E+00	4.84E+00	5.38E-01	2.86E-01
FR-485-TH230-Bulk 2	4/13/99	26.46	0.2838	0	6.67E-01	2.35E+00	5.24E-05	1.07E+00	1.66E-01
FR-515-TH-Bulk 1 Run 3	4/18/99	28.42	0.4847	23	1.43E+00	1.28E+01	5.25E+01	5.83E+00	1.99E-01
FR-515-TH230-Bulk 1 Run 3	4/18/99	28.42	0.4847	23	6.35E-01	5.70E+00	1.27E-04	2.59E+00	2.36E-01
FR-515-TH-Bulk 2	3/6/99	11.51	1.358	24	5.98E-01	1.83E+00	7.51E+00	8.34E-01	2.59E-01
FR-515-TH230-Bulk 2	3/6/99	11.51	1.358	24	7.47E-02	2.29E-01	5.11E-06	1.04E-01	3.89E-01
FR-530-TH-Bulk 1	3/6/99	21.75	0.557	95	2.26E-01	4.25E-01	1.74E+00	1.93E-01	2.88E-01
FR-530-TH230-Bulk 1	3/6/99	21.75	0.557	95	8.68E-01	1.64E+00	3.65E-05	7.44E-01	1.27E-01
FR-530-TH-Bulk 2	3/17/99	37.71	0.557	1	4.12E-02	7.22E+00	2.96E+01	3.28E+00	5.32E-01
FR-530-TH230-Bulk 2	3/17/99	37.71	0.557	1	3.65E-02	6.41E+00	1.43E-04	2.91E+00	2.33E-01

Thorium Concentrations

Decay Constants	^{232}Thorium	^{230}Thorium
Decay Constants (per min)	9.414E-17	1.71E-11
Molecular mass (g/Mole)	232	230
Avagadro's # (atoms/mole)	6.02E+23	
DPM/pCi	2.20E+00	

Bulk 1 = Carbonate Portion
Bulk 2 = Silicate Portion

-	**Date Counted**	**Total Recovery (%)**	**Initial Mass sampled**	**% Lost**	**DPM**	**DPM/g**	**ppm**	**pCi/g**	**total error**
OK-55-Th-BULK 1	3/1/99	27.09	0.4995	37	1.95E+00	1.07E+01	4.39E+01	4.87E+00	1.94E-01
OK-55-Th230-BULK 1	3/1/99	27.09	0.4995	37	8.01E-01	4.40E+00	9.82E-05	2.00E+00	2.31E-01
OK-55-Th-BULK 2	4/15/99	24.80	0.5159	61	2.01E-01	6.39E-01	2.62E+00	2.91E-01	2.69E-01
OK-55-Th230-BULK 2	4/15/99	24.80	0.5159	61	1.96E-01	6.23E-01	1.39E-05	2.83E-01	1.98E-01
OK-100-Th Bulk 1 Duplicate	3/16/99	36.10	0.633	55.6	7.76E-01	2.02E+00	8.26E+00	9.17E-01	2.27E-01
OK-100-Th230 Bulk 1 Duplicate	3/16/99	36.10	0.633	55.6	1.63E-01	4.23E-01	9.43E-06	1.92E-01	2.72E-01
OK-100-Th Bulk 1 (run 2)	4/2/99	40.73	0.633	55.6	7.90E-01	2.21E+00	9.06E+00	1.01E+00	1.34E-01
OK-100-Th230 Bulk 1(run 2)	4/2/99	40.73	0.633	55.6	1.03E-01	2.90E-01	6.47E-06	1.32E-01	1.73E-01
OK-100-Th Bulk 2 (run 2)	4/2/99	18.58	0.633	39	1.39E-01	5.56E-01	2.28E+00	2.53E-01	4.35E-01
OK-100-Th230 Bulk 2 (run 2)	4/2/99	18.58	0.633	39	4.88E-01	1.95E+00	4.36E-05	8.88E-01	1.74E-01
OK-230-Th-Bulk 1 Run 2	4/10/99	31.91	0.5338	25	1.85E+00	1.39E+01	5.68E+01	6.31E+00	1.31E-01
OK-230-Th230 Bulk 1Run 2	4/10/99	31.91	0.5338	25	7.85E-01	5.88E+00	1.31E-04	2.67E+00	1.52E-01
OK-230-Th-Bulk 2	3/31/99	28.02	0.5338	71	9.75E-01	2.57E+00	1.05E+01	1.17E+00	2.27E-01
OK-230-Th230 Bulk 2	3/31/99	28.02	0.5338	71	9.17E-01	2.42E+00	5.40E-05	1.10E+00	1.87E-01
LLB 105 TH Bulk 1 Run 2	4/28/99	30.16	0.43	32	1.80E+00	1.31E+01	5.36E+01	5.95E+00	1.34E-01
LLB 105 Th230 Bulk 1 Run2	4/28/99	30.16	0.43	32	9.41E-01	6.84E+00	1.53E-04	3.11E+00	1.45E-01
LLB 105 TH Bulk 2 Run 2	4/22/99	28.54	0.434	67	1.00E+00	3.47E+00	1.42E+01	1.58E+00	1.27E-01
LLB 105 Th230 Bulk 2 Run2	4/22/99	28.54	0.434	67	1.15E+00	4.00E+00	8.94E-05	1.82E+00	9.81E-02
LLB 125 TH Bulk 1 Run 2	4/22/99	29.65	0.434	29	1.72E+00	1.36E+01	5.57E+01	6.19E+00	9.68E-02
LLB 125 Th230 Bulk 1 Run2	4/22/99	29.65	0.434	29	1.20E+00	9.49E+00	2.12E-04	4.31E+00	9.52E-02
LLB 125 TH Bulk 2 Run 2	4/26/99	21.80	0.434	67	6.04E-01	2.08E+00	8.50E+00	9.44E-01	1.88E-01
LLB 125 Th230 Bulk 2 Run2	4/26/99	21.80	0.434	67	1.17E+00	4.03E+00	9.00E-05	1.83E+00	1.13E-01

Radium Concentrations							
Decay Constants	^{222}Rn	^{226}Ra					
Decay Constants (per min)	3.453E-07	8.13E-10					
Molecular mass (g/Mole)	222	226					
Avagadro's # (atoms/mole)	6.02E+23						
DPM/pCi	2.20E+00						
	Date Counted	**DPM/g**	**ppm**	**pCi/g 226Ra**	**226Ra ppm**	**Counts**	**total Error**
Neda bulk-^{222}Rn	10/27/98	1.55E+00	1.66E-09	7.06E-01	7.17E-07	1.85E+03	7.13E-02
Neda SC-^{222}Rn	10/27/98	2.02E+00	2.16E-09	9.18E-01	9.33E-07	3.03E+03	5.65E-02
Rn-04-231-Bulk	12/7/98	8.07E+00	8.62E-09	3.67E+00	3.73E-06	1.86E+03	7.11E-02
Rn-02-250.8-Bulk	12/1/98	8.28E-01	8.84E-10	3.76E-01	3.82E-07	1.84E+03	7.15E-02
Rn-03-271-Bulk	12/1/98	5.30E+00	5.66E-09	2.41E+00	2.45E-06	1.72E+03	7.39E-02
Rn-05-287-Bulk	12/7/98	9.20E+00	9.82E-09	4.18E+00	4.25E-06	1.33E+03	8.36E-02
Rn-317-Bulk	2/10/99	1.08E+00	1.15E-09	4.90E-01	4.98E-07	3.51E+03	5.28E-02
Rn-331-Bulk	12/7/98	9.80E-01	1.05E-09	4.45E-01	4.53E-07	2.54E+03	6.14E-02
Rn-331-Bulk Duplicate	2/10/99	1.08E+00	1.15E-09	4.91E-01	4.99E-07	2.40E+03	6.31E-02
Rn-08-345.5-Bulk	2/8/99	6.30E+00	6.73E-09	2.86E+00	2.91E-06	2.09E+03	6.73E-02
Rn-06-358.6-Bulk	12/4/98	1.18E+01	1.26E-08	5.35E+00	5.44E-06	9.09E+03	3.49E-02
Rn-02-379.5-Bulk	12/3/98	1.07E+01	1.14E-08	4.86E+00	4.94E-06	2.01E+03	6.86E-02
Rn-05-392-Bulk	12/4/98	3.50E+00	3.74E-09	1.59E+00	1.62E-06	2.91E+03	5.76E-02
Minooka # 1 Filter paper (dpm/L)	2/2/99	2.04E+00	2.18E-09	9.27E-01	9.42E-07	2.88E+03	5.79E-02
Minooka # 2 Filter paper	2/8/99	2.94E-01	3.14E-10	1.34E-01	1.36E-07	3.51E+03	5.28E-02
Minooka # 3 Filter paper	2/8/99	4.64E-01	4.96E-10	2.11E-01	2.14E-07	2.59E+03	6.08E-02
Minooka # 4 Filter paper	2/8/99	1.21E+00	1.29E-09	5.50E-01	5.58E-07	4.39E+03	4.77E-02
Minooka # 5 Filter paper	2/8/99	1.78E+00	1.90E-09	8.07E-01	8.20E-07	3.11E+03	5.58E-02
FR-320	3/16/99	1.43E+00	1.53E-09	6.50E-01	6.60E-07	4.75E+03	4.60E-02
FR-415	3/17/99	1.95E+00	2.08E-09	8.86E-01	9.01E-07	2.22E+03	6.54E-02
FR485	3/21/99	5.81E+00	6.20E-09	2.64E+00	2.68E-06	5.33E+03	4.37E-02
FR-515	3/18/99	3.08E+00	3.29E-09	1.40E+00	1.42E-06	2.84E+03	5.83E-02
FR-530	3/18/99	4.89E-01	5.22E-10	2.22E-01	2.26E-07	8.32E+02	1.05E-01
OK 55	5/20/99	2.45E+00	2.62E-09	1.11E+00	1.13E-06	1.76E+03	7.30E-02
OK 100	4/22/99	2.10E+00	2.24E-09	9.55E-01	9.70E-07	3.58E+03	5.24E-02
OK 230	4/22/99	4.08E+00	4.35E-09	1.85E+00	1.88E-06	2.54E+03	6.14E-02
LLB 105	5/20/99	3.02E+00	3.23E-09	1.37E+00	1.39E-06	3.44E+03	5.33E-02
LLB 125	5/21/99	1.97E+00	2.10E-09	8.95E-01	9.10E-07	9.78E+03	3.38E-02

Appendix B: Water quality data taken from wells in Pewaukee, New Berlin and Brookfield showing chemical trends over time. Shaded values are those that affect the corresponding radiometric trends.

Pewaukee #4- 1978

ION	CONC. (mg/L)	MOLAR EQUIV. (meq/L)	PERCENT MEQUIV
Ca	65.0	3.24	53
Mg	29.0	2.39	39
Na	11.0	0.48	8
K		0.00	0
Fe2+			
pH	7.4		
HCO3	234.0	3.84	73
Cl	4.0	0.11	2
SO4	63.0	1.31	25
NO3			
OH			

ELECTRICAL BALANCE (%)	8
IONIC STRENGTH (mM)	9
TOTAL CONC. (mg/L)	407

Pewaukee #4- 1989

ION	CONC. (mg/L)	MOLAR EQUIV. (meq/L)	PERCENT MEQUIV
Ca	55.0	2.74	53
Mg	24.0	1.98	38
Na	11.0	0.48	9
K		0.00	0
Fe2+			
pH	8.0		
HCO3	237.0	3.89	71
Cl	5.2	0.15	3
SO4	71.0	1.48	27
NO3			
OH			

ELECTRICAL BALANCE (%)	3
IONIC STRENGTH (mM)	9
TOTAL CONC. (mg/L)	403

New Berlin #8 - 1983

ION	CONC. (mg/L)	MOLAR EQUIV. (meq/L)	PERCENT MEQUIV
Ca	140.0	6.98	72
Mg	24.0	1.98	20
Na	16.0	0.70	7
K		0.00	0
Fe2+			
pH	7.4		
HCO3	246.0	4.03	41
Cl	9.0	0.25	3
SO4	270.0	5.62	57
NO3			
OH			

ELECTRICAL BALANCE (%)	1
IONIC STRENGTH (mM)	17
TOTAL CONC. (mg/L)	705

New Berlin #8 - 1986

ION	CONC. (mg/L)	MOLAR EQUIV. (meq/L)	PERCENT MEQUIV
Ca	173.0	8.63	76
Mg	25.0	2.06	18
Na	16.0	0.70	6
K		0.00	0
Fe2+			
pH	7.7		
HCO3	242.0	3.97	37
Cl	9.0	0.25	2
SO4	310.0	6.45	60
NO3			
OH			

ELECTRICAL BALANCE (%)	3
IONIC STRENGTH (mM)	20
TOTAL CONC. (mg/L)	775

New Berlin #8 - 1994

ION	CONC. (mg/L)	MOLAR EQUIV. (meq/L)	PERCENT MEQUIV
Ca	300.0	14.96	83
Mg	26.0	2.14	12
Na	17.0	0.74	4
K	8.0	0.20	1
Fe2+			
pH	7.0		
HCO3	265.0	4.34	29
Cl	12.0	0.34	2
SO4	501.0	10.43	69
NO3			
OH			

ELECTRICAL BALANCE (%)	9
IONIC STRENGTH (mM)	30
TOTAL CONC. (mg/L)	1129

Brookfield #24 - 1991

ION	CONC. (mg/L)	MOLAR EQUIV. (meq/L)	PERCENT MEQUIV
Ca	63.0	3.14	58
Mg	22.0	1.81	34
Na	10.0	0.43	8
K		0.00	0
Fe2+			
pH	7.9		
HCO3	96.0	1.57	32
Cl	8.0	0.23	5
SO4	150.0	3.12	63
NO3			
OH			

ELECTRICAL BALANCE (%)	5
IONIC STRENGTH (mM)	9
TOTAL CONC. (mg/L)	349

Brookfield #24 - 1991

ION	CONC. (mg/L)	MOLAR EQUIV. (meq/L)	PERCENT MEQUIV
Ca	61.0	3.04	55
Mg	25.0	2.06	37
Na	11.0	0.48	9
K		0.00	0
Fe2+			
pH	7.9		
HCO3	140.0	2.30	52
Cl	7.5	0.21	5
SO4	91.0	1.89	43
NO3			
OH			

ELECTRICAL BALANCE (%)	2
IONIC STRENGTH (mM)	9
TOTAL CONC. (mg/L)	336

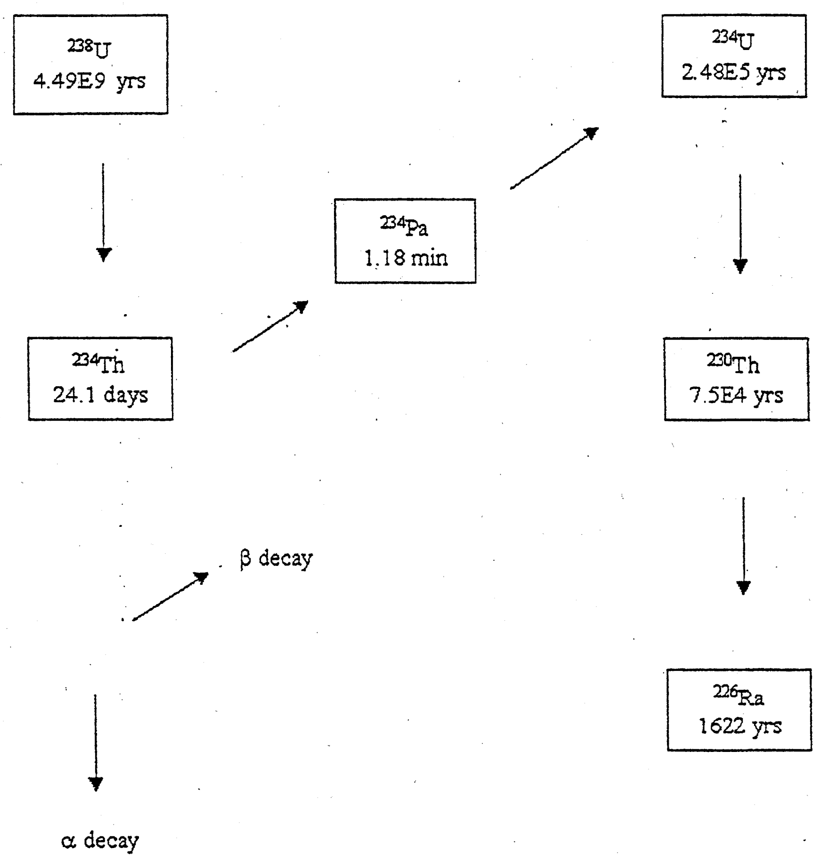

Figure 1. ^{238}U decay series. Half-lives are indicated beneath each isotope.

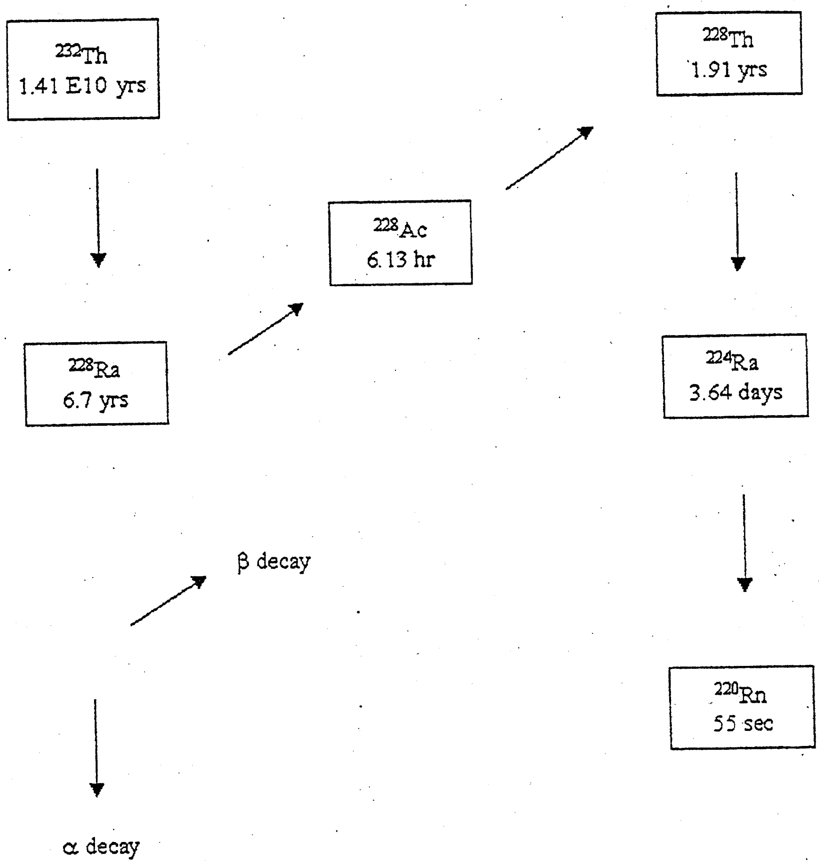

Figure 2. ^{232}Th decay series. Half-lives are indicated beneath each isotope.

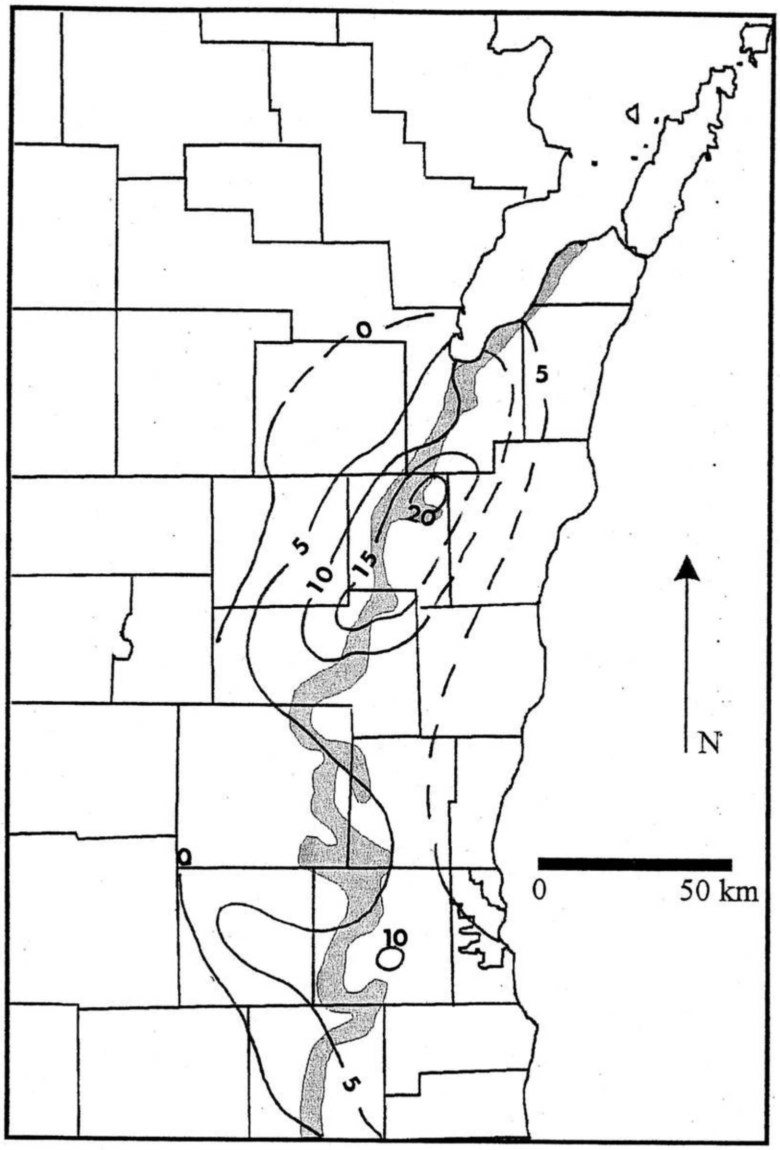

Figure 3. Average total radium concentrations detected in public water supply systems 1986 to 1990. Contours are isoconcentration lines in pC/L. The Makoqueta Shale subcrop pattern is shown in gray.

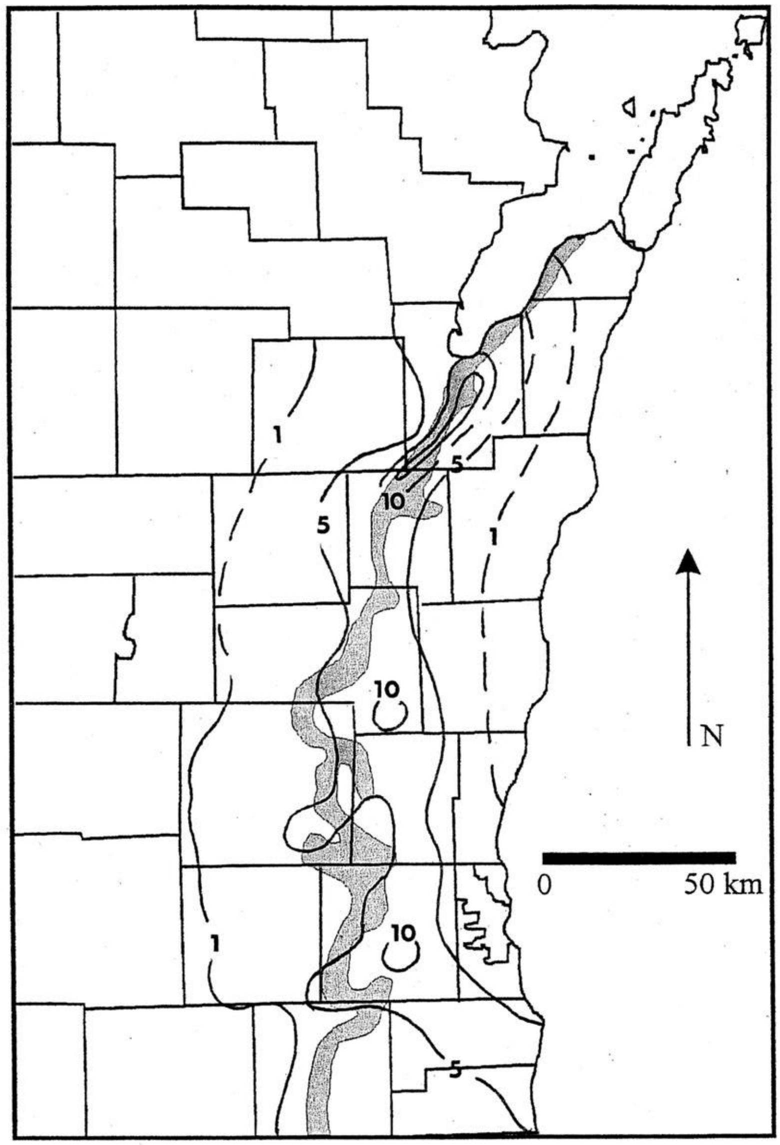

Figure 4. Average total radium concentrations detected in public water supply systems 1991 to 1995. Contours are isoconcentration lines in pC/L. The Makoqueta Shale subcrop pattern is shown in gray.

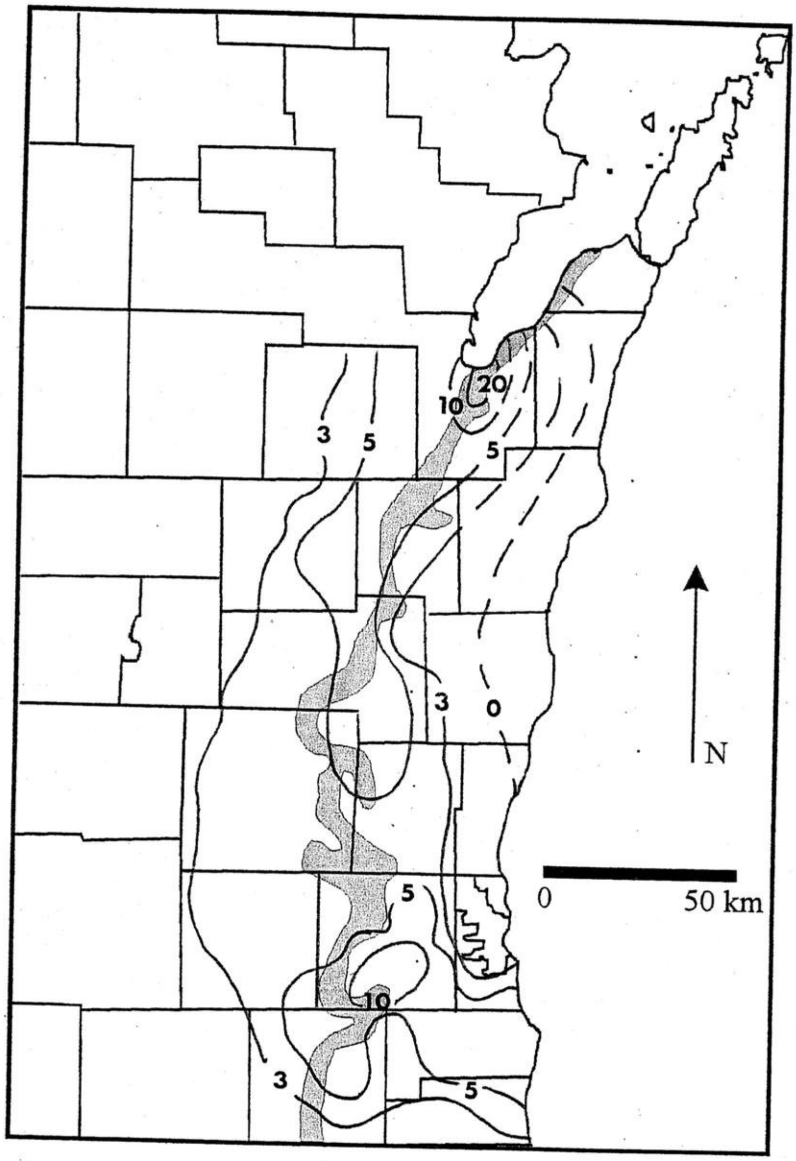

Figure 5. Average total radium concentrations detected in public water supply systems 1996 to 2000. Contours are isoconcentration lines in pC/L. The Makoqueta Shale subcrop pattern is shown in gray.

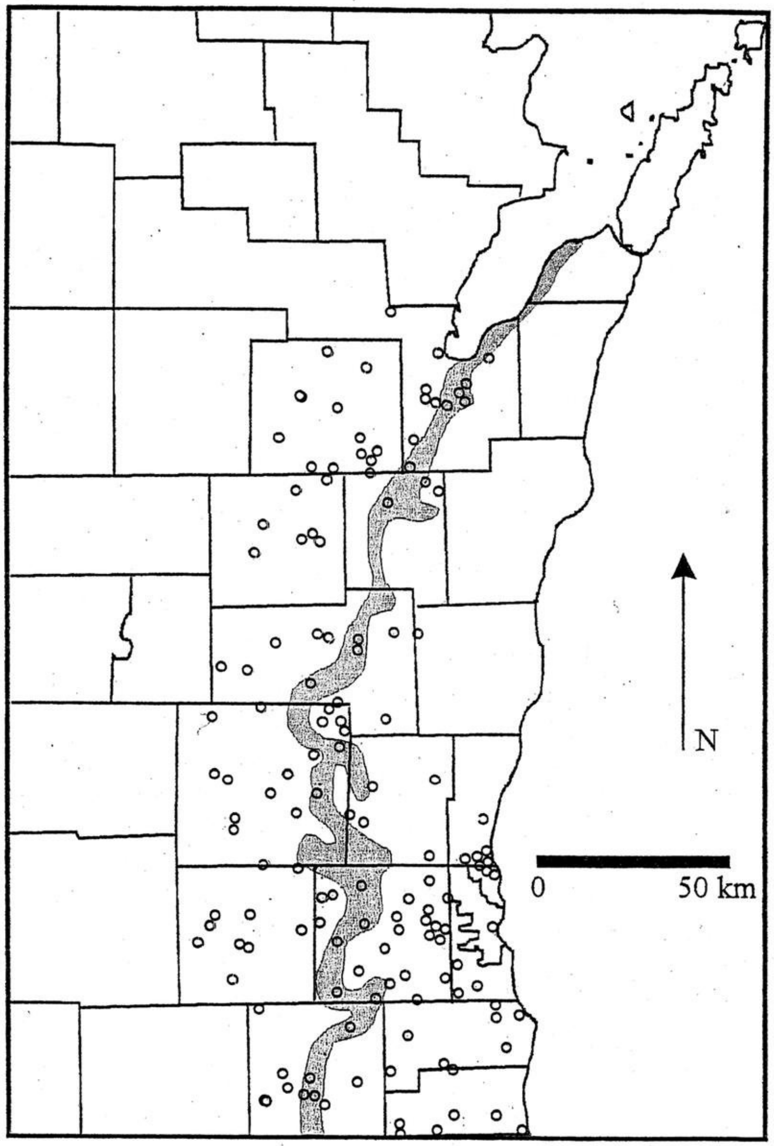

Figure 6. Public water supply systems used in the generation of both radium and gross alpha distribution plots. The Makoqueta Shale subcrop pattern is shown in gray.

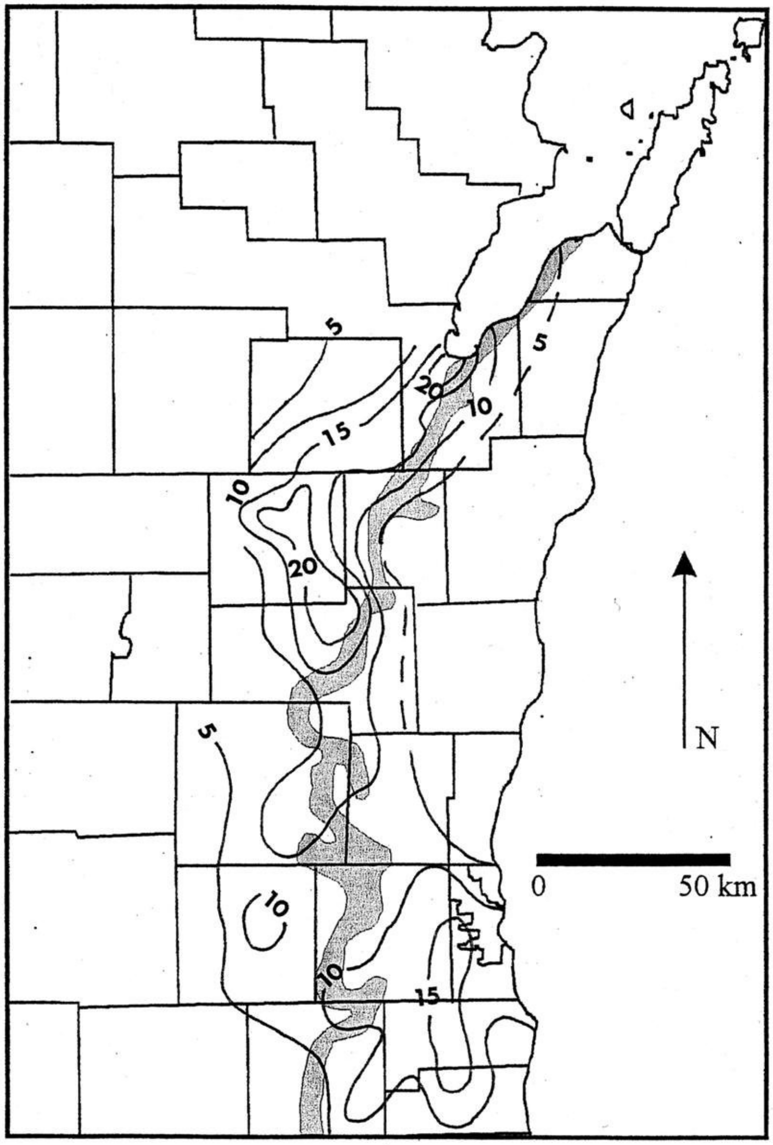

Figure 7. Average gross alpha concentrations detected in public water supply systems 1986 to 1990. Contours are isoconcentration lines in pC/L. The Makoqueta Shale subcrop pattern is shown in gray.

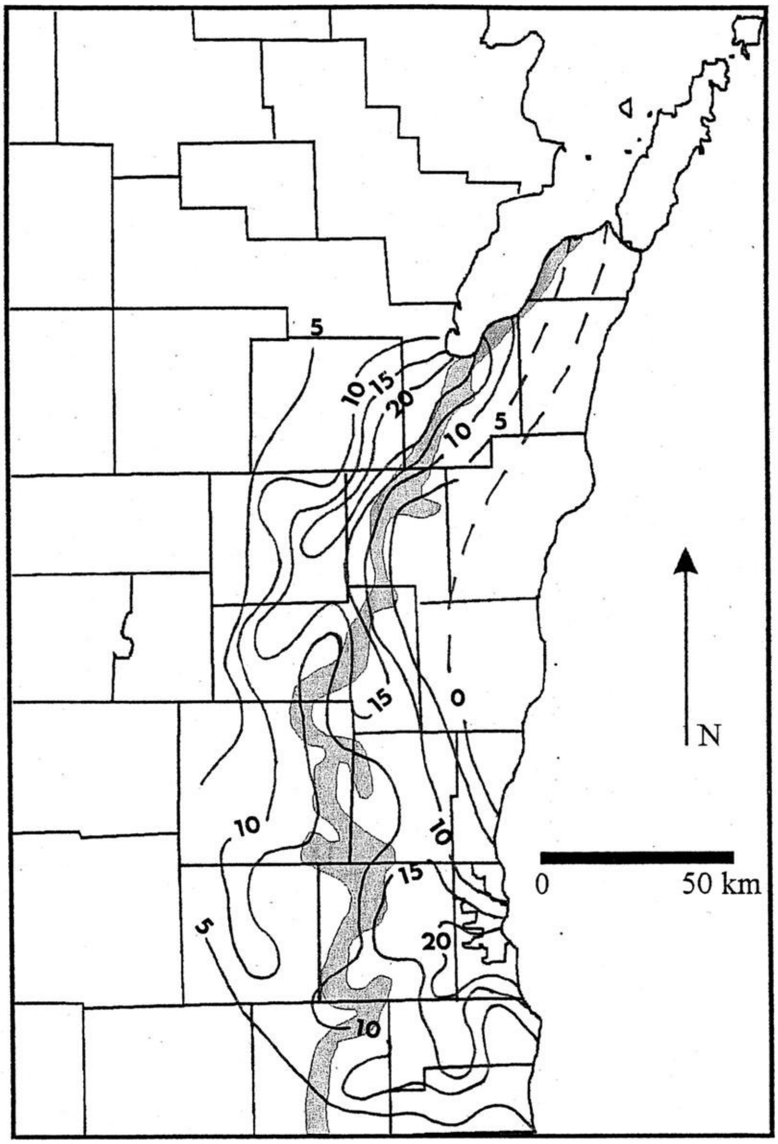

Figure 8. Average gross alpha concentrations detected in public water supply systems 1991 to 1995. Contours are isoconcentration lines in pC/L. The Makoqueta Shale subcrop pattern is shown in gray.

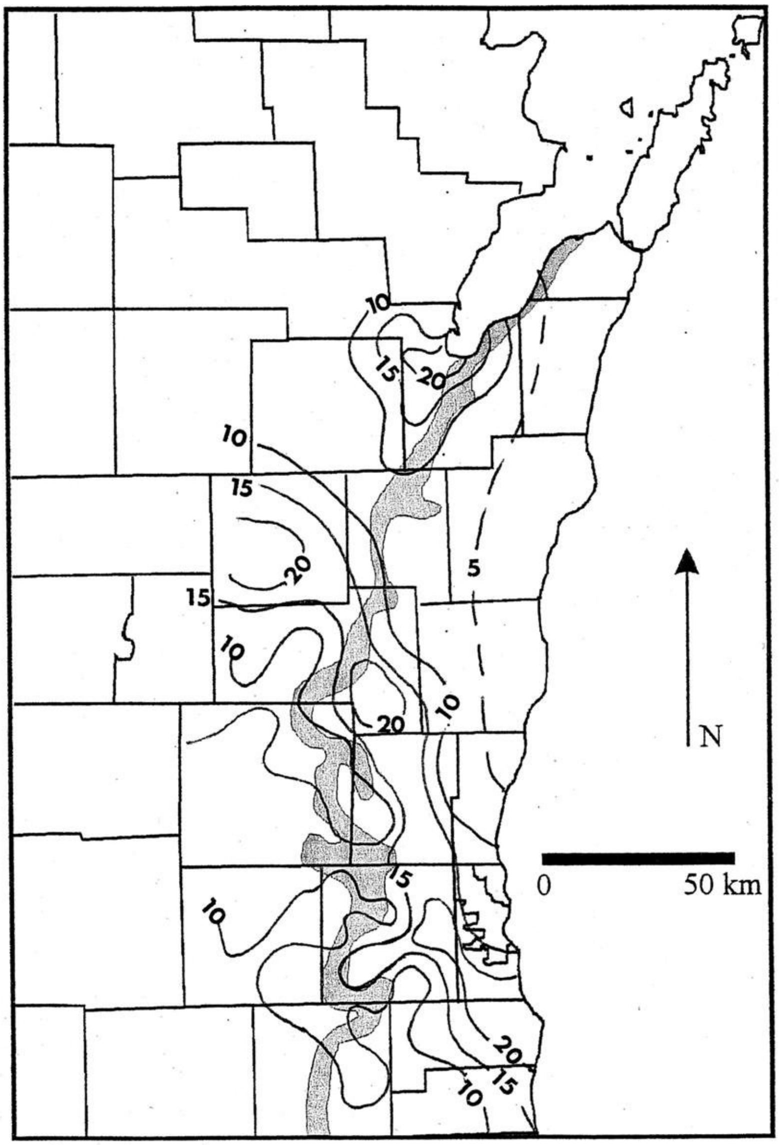

Figure 9. Average gross alpha concentrations detected in public water supply systems 1996 to 2000. Contours are isoconcentration lines in pC/L. The Makoqueta Shale subcrop pattern is shown in gray.

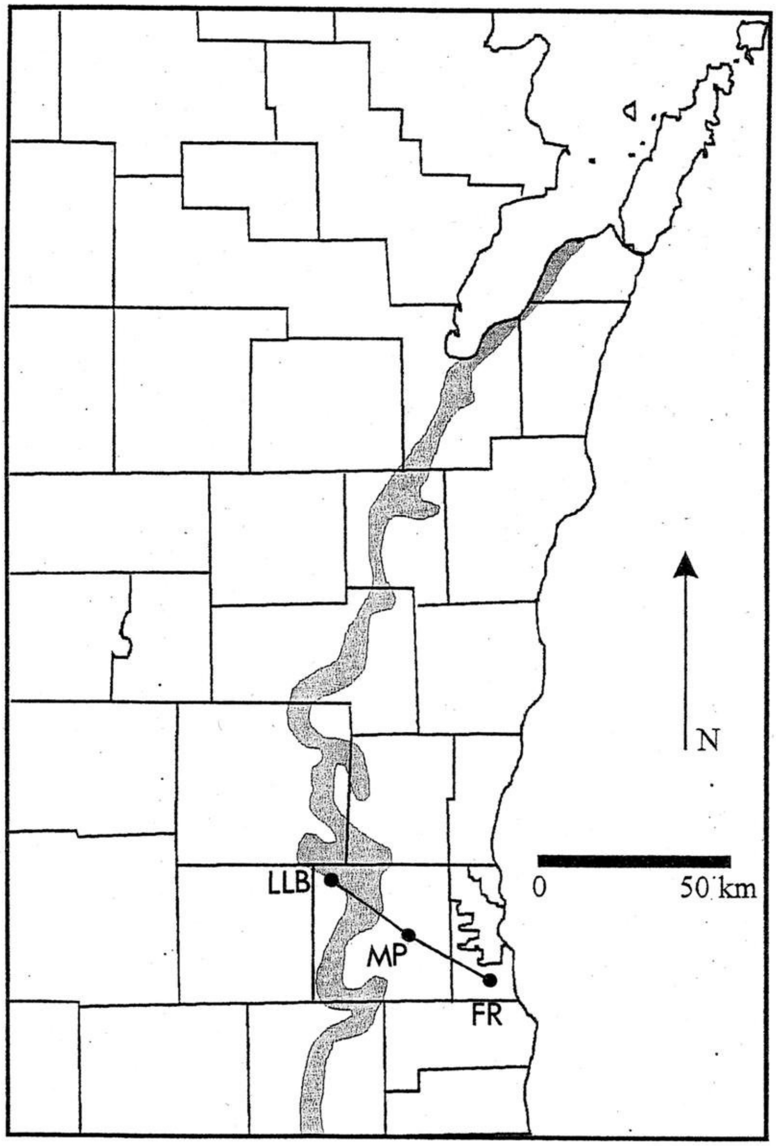

Figure 10. Location of the transect consisting of the Fanklin #5 (FR), Minooka Park (MP) and Lac la Belle (LLB) wells. The Makoqueta Shale subcrop pattern is shown in gray.

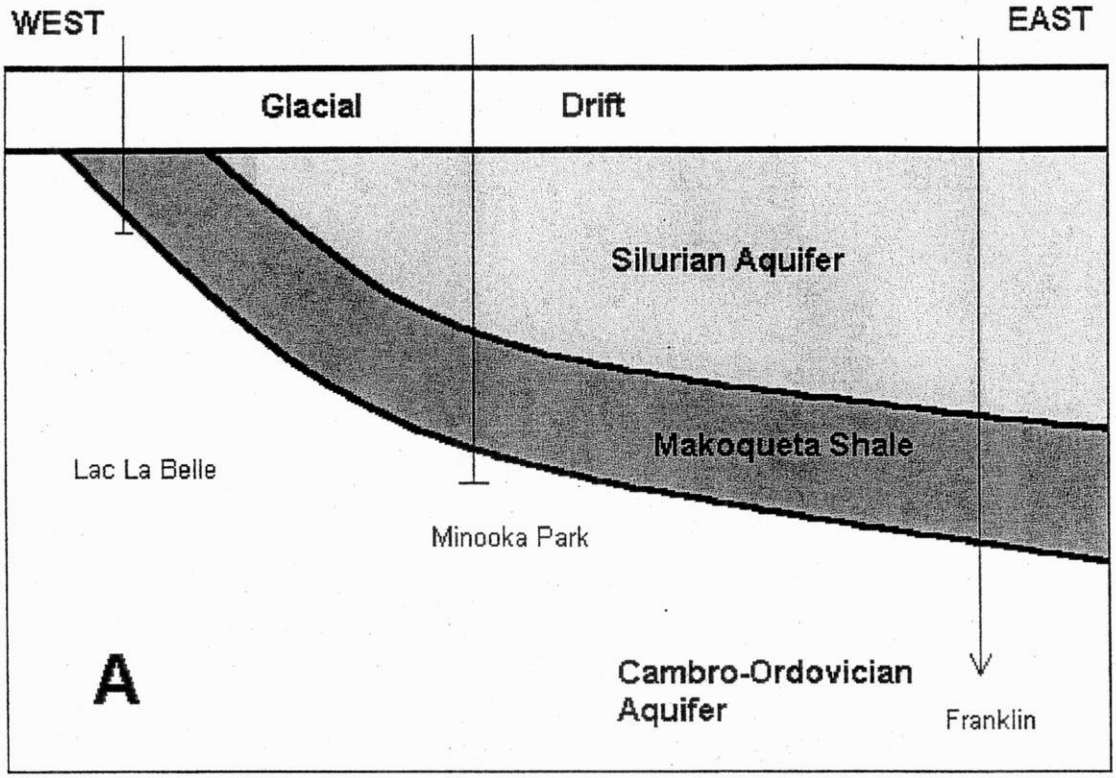

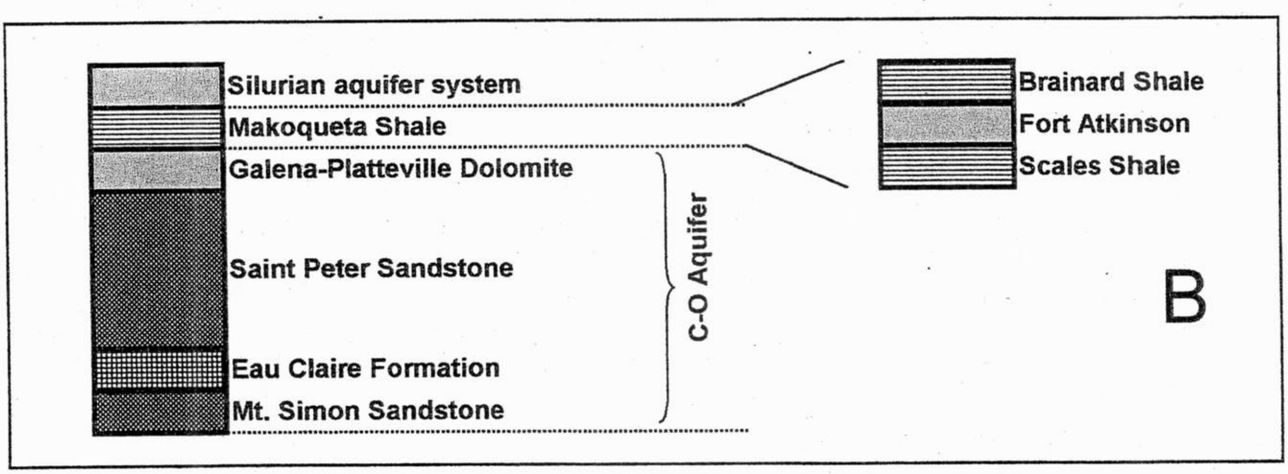

Figure 11. A) Diagrammatic representation of the overall stratigraphy along the Lac la Belle - Franklin transect. B) Diagrammatic representation of the gross stratigraphy in the study area.

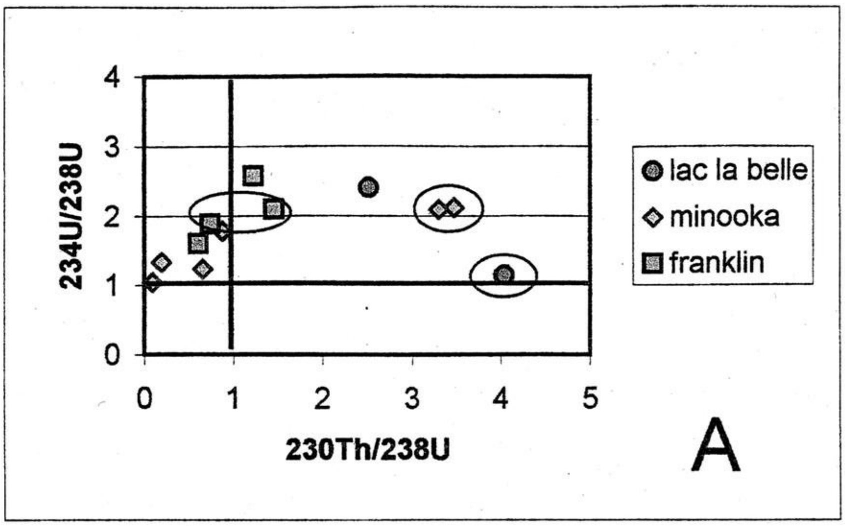

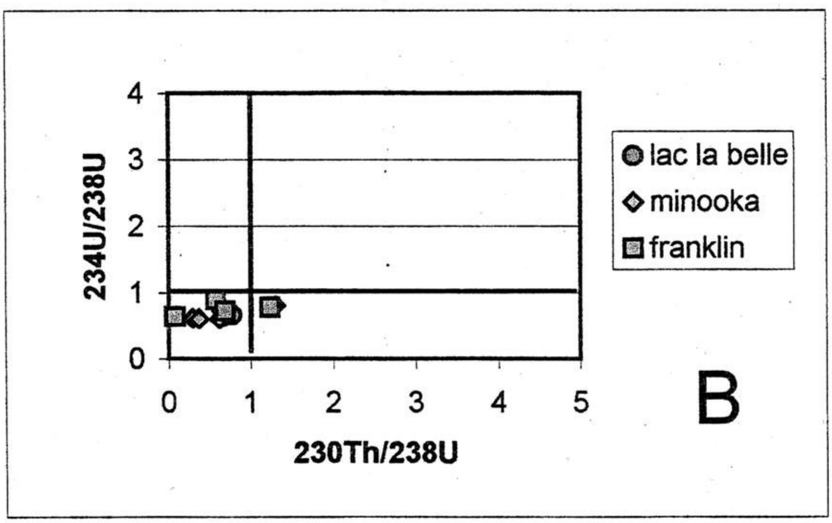

Figure 12. Activity ratio cross-plots for the parent isotopes of radium in the solids of the Makoqueta Shale. A) Values measured in the surface coatings fraction. Circled points represent samples taken from the Scales Shale. B) Values measured in the silicate fraction.

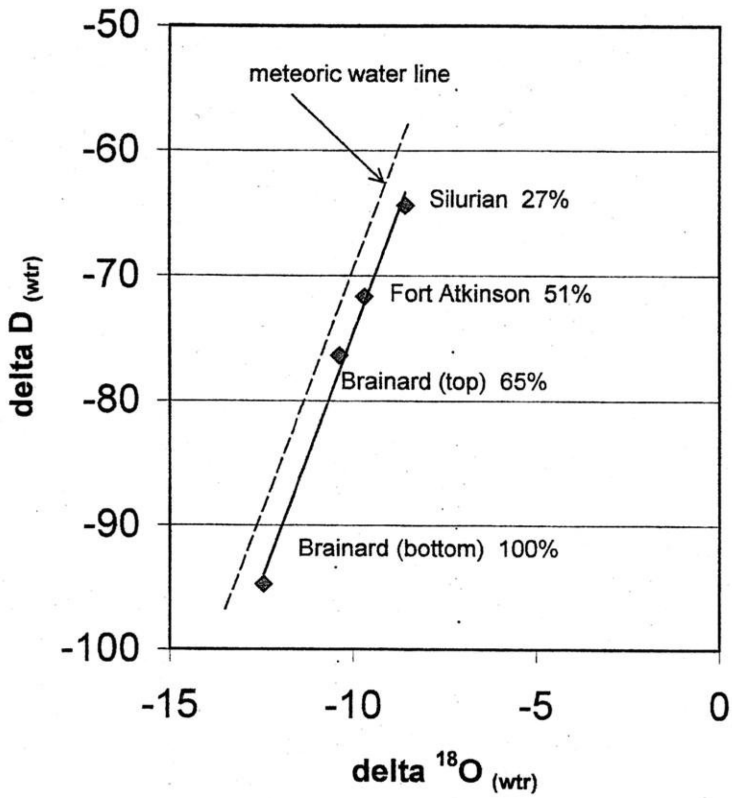

Figure 13. Plot of the stable isotopic signature of water taken from the Minooka Park well. Meteoric water line is that of Dansgaard (1964). Solid line is the best fit line through the data points. Percent values represent the % Pleistocene component of each particular water. Figure is modified after Eaton and Bradbury (1998).

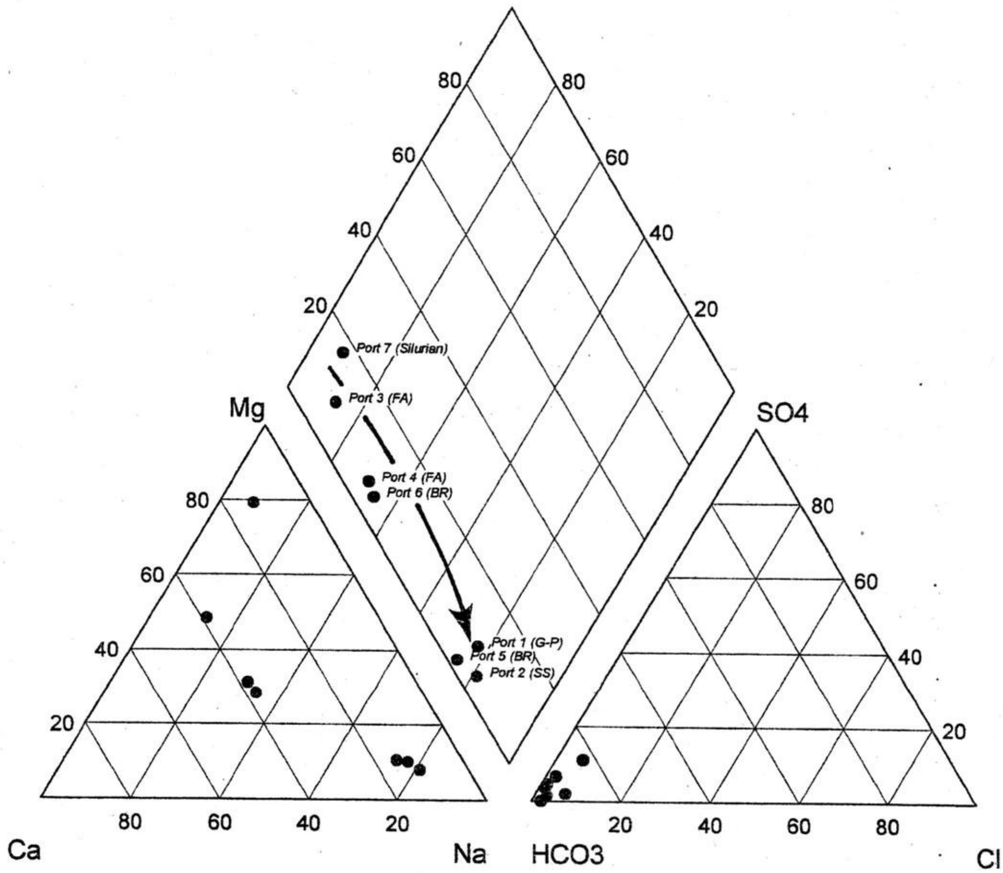

Figure 14. Piper diagram of waters taken from the Minooka Park well. Arrow shows the trend of geochemical evolution over time. BR = Brainard Shale water. FA = Fort Atkinson water. G-P = Galena Platteville water. Silurian = Silurian Dolomite water. SS = Scales Shale water.

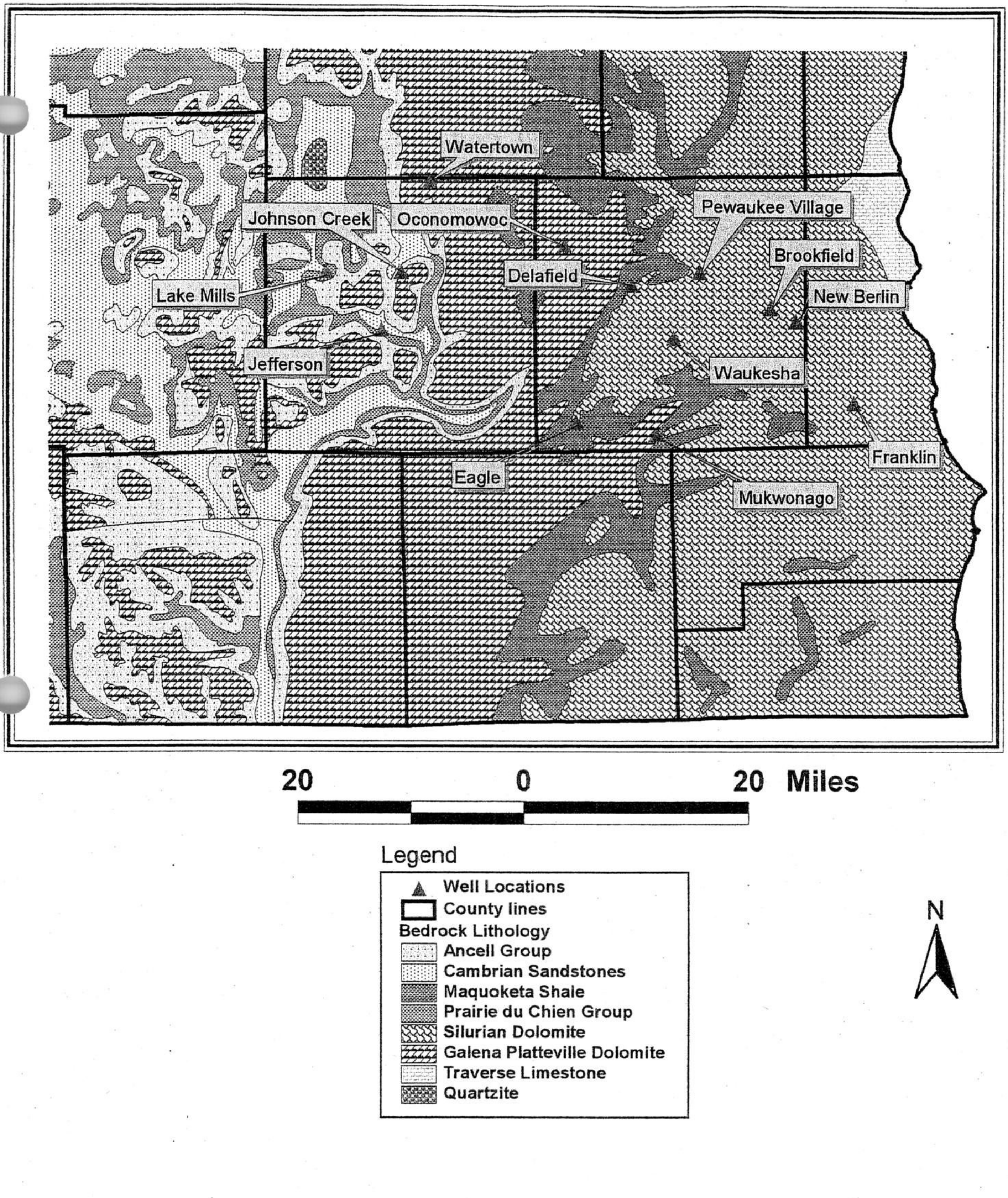

Figure 15: Location map for the municipal water supplies that were studied in detail. Data were obtained from these municipalities from the period 1997 through 1999.

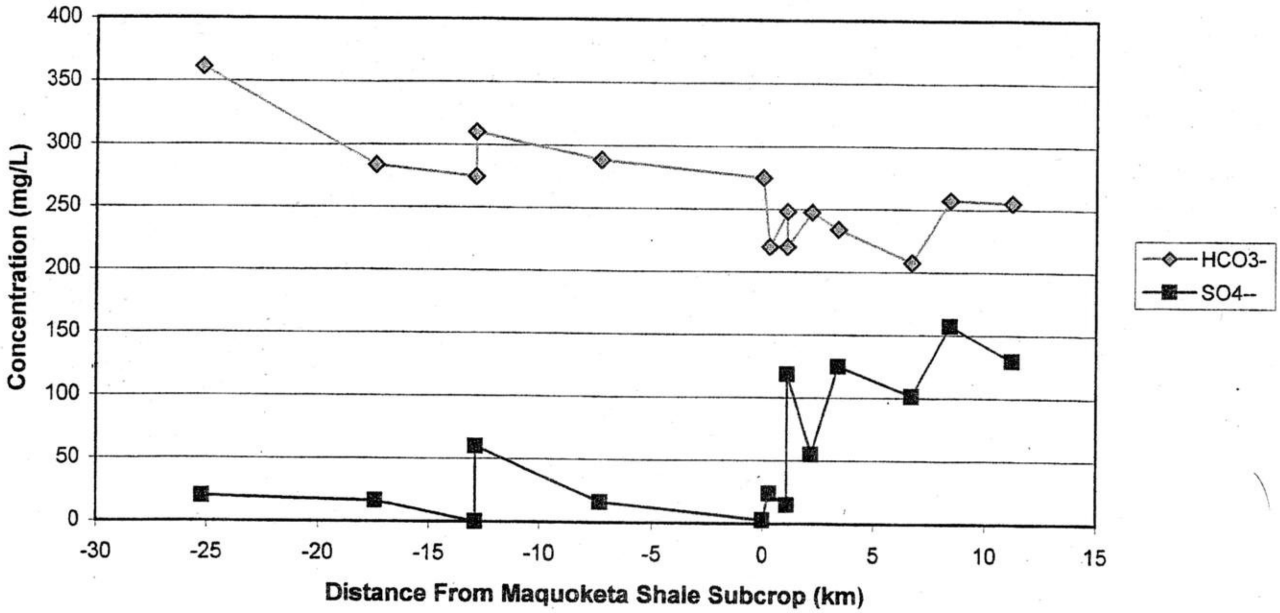

Figure 16. HCO_3 and SO_4 content of Cambro-Ordovician water in southeastern Wisconsin. Distance scale is given in kilometers west (negative values) and east (positive values) of the Makoqueta subcrop along the groundwater flowpath.

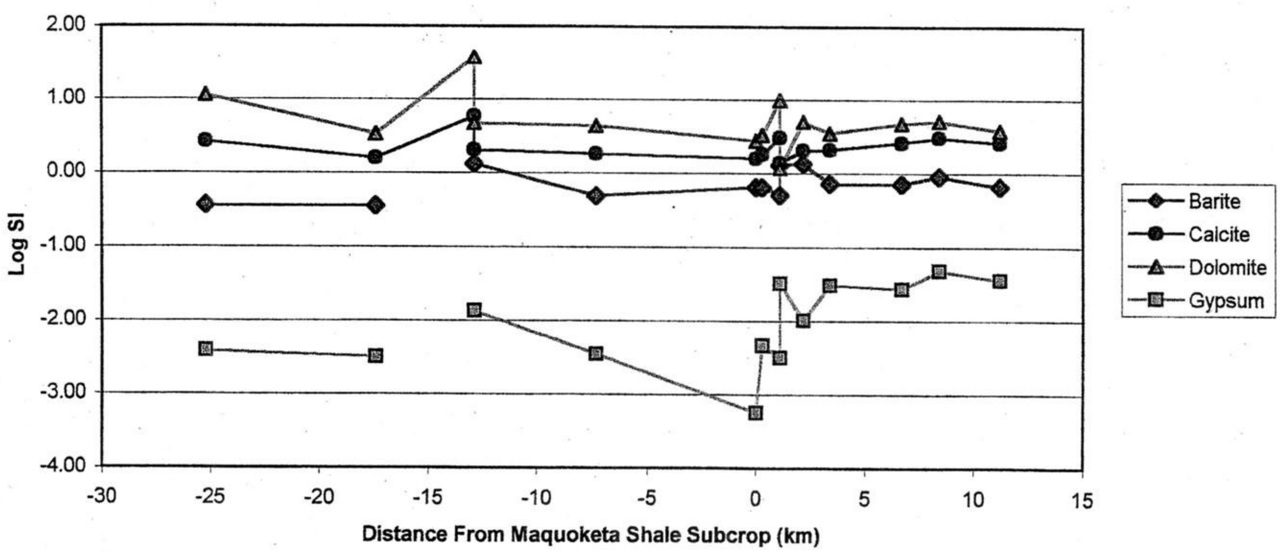

Figure 17. Saturation indices for barite, gypsum, calcium, and dolomite in Cambro-Ordovician water of southeastern Wisconsin. Distance scale is given in kilometers west (negative values) and east (positive values) of the Makoqueta subcrop along the groundwater flowpath.

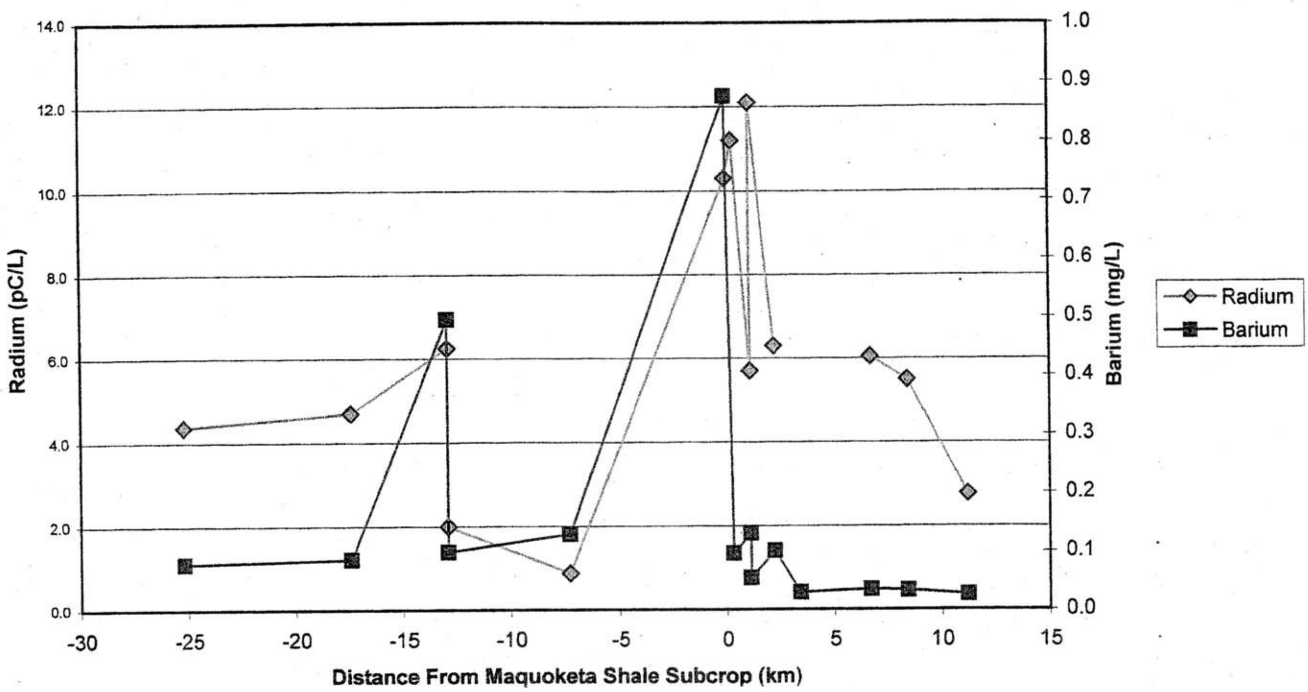

Figure 18. Radium and barium concentrations in the Cambro-Ordovician water of southeastern Wisconsin. Distance scale is given in kilometers west (negative values) and east (positive values) of the Makoqueta subcrop along the groundwater flowpath.

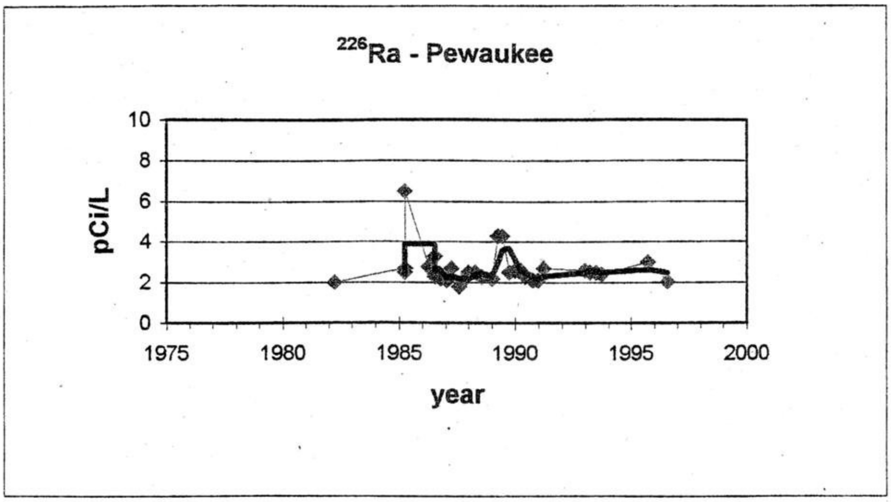

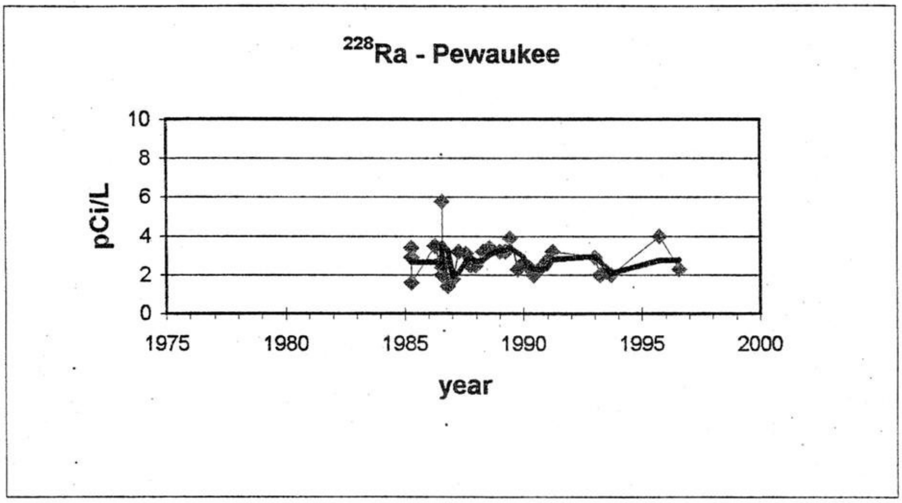

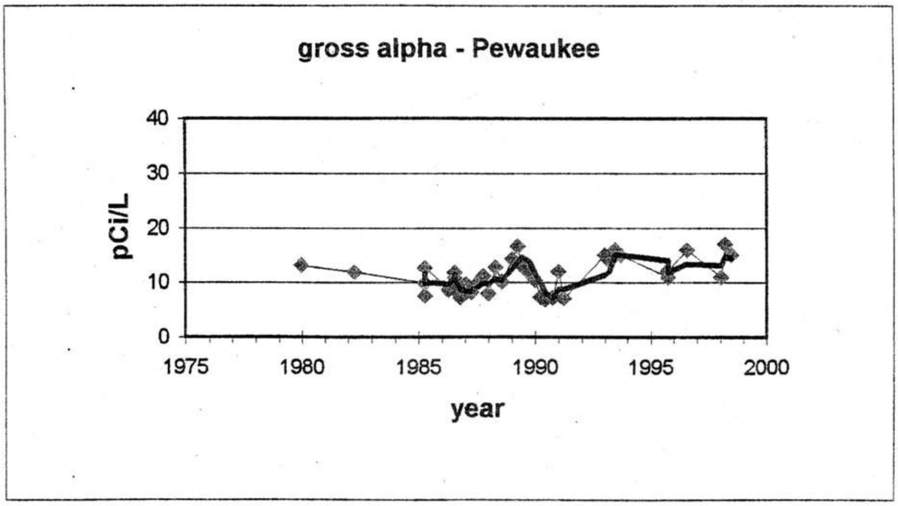

Figure 19. Temporal trend in the radiometric content of the Pewaukee municipal water supply. Heavy black line is the three-year moving average.

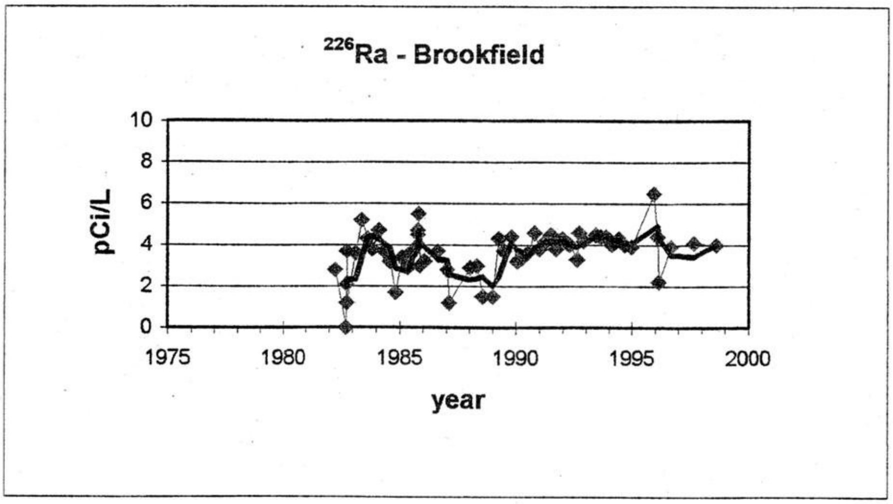

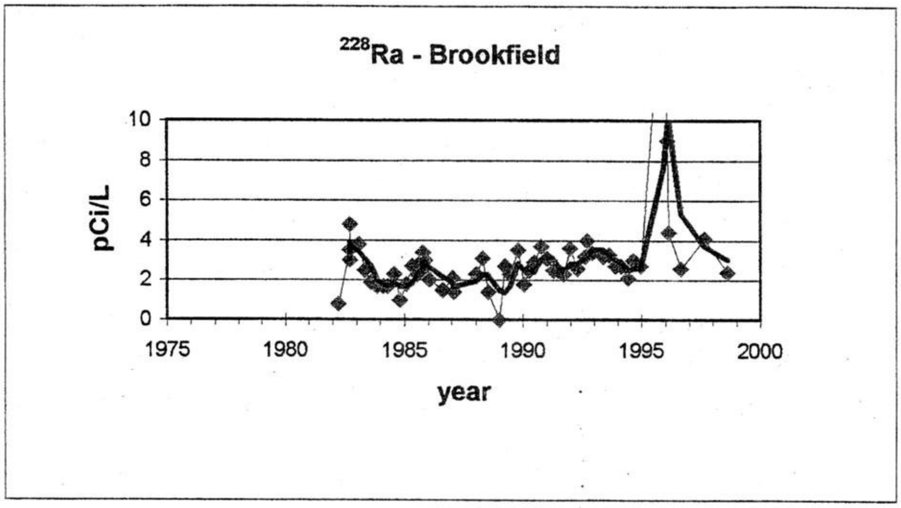

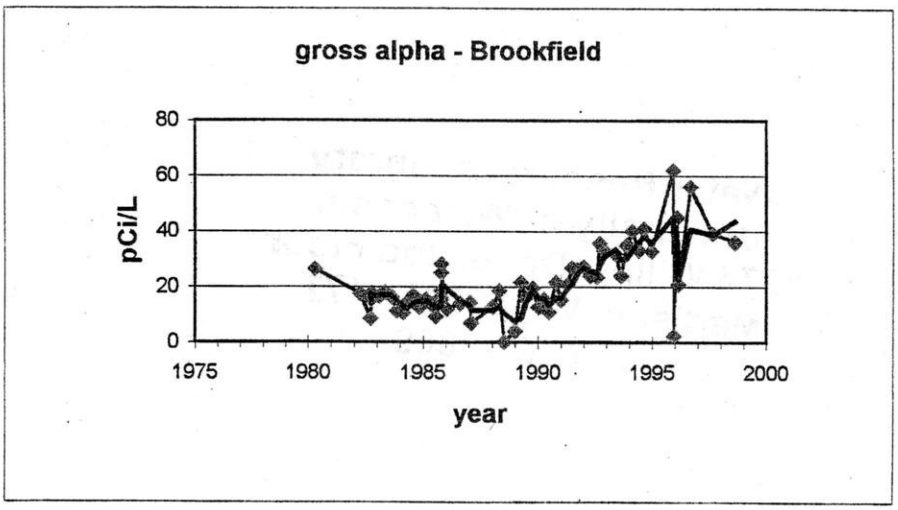

Figure 20. Temporal trend in the radiometric content of the Brookfield municipal water supply. Heavy black line is the three-year moving average.